Materials Science in Semiconductor Processing 180 (2024) 108559

Contents lists available at ScienceDirect

Materials Science in Semiconductor Processing

journal homepage: www.elsevier.com/locate/mssp

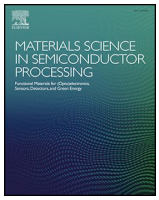

Perspective

A review of ultra-short pulse laser micromachining of wide bandgap semiconductor materials: SiC and GaN

Keran Jiang [a], Peilei Zhang [a,*], Shijie Song [a], Tianzhu Sun [b,**], Yu Chen [c], Haichuan Shi [a], Hua Yan [a], Qinghua Lu [a], Guanglong Chen [d]

[a] School of Materials Science and Engineering, Shanghai University of Engineering Science, Shanghai, 201620, China
[b] Warwick Manufacturing Group (WMG), University of Warwick, Coventry CV4 7AL, UK
[c] Amplitude Shanghai Laser Technology Company Ltd., Shanghai, 200127, China
[d] School of Mathematics, Physics and Statistics, Shanghai University of Engineering Science, Shanghai, 201620, China

ARTICLE INFO

Keywords:
Wide bandgap semiconductor materials
Ultra-short pulse laser
Silicon carbide
Gallium nitride
Picosecond laser
Femtosecond laser

ABSTRACT

Wide bandgap (WBG) materials have excellent semiconductor and physicochemical properties and are emerging materials. Silicon carbide (SiC) and gallium nitride (GaN), two representatives of third-generation semiconductor materials, can be used in high temperature, high voltage, high frequency, and high power applications. However, both materials are difficult to machine due to their brittle and hard properties. Laser processing is a suitable processing method, and in particular the unique non-thermal properties of ultra-short pulse laser processing have led to a wide range of applications in a variety of materials including ceramics, metals and biological tissues. WBG materials are third-generation semiconductor materials with broad application prospects in the semiconductor industry, but there are relatively few summarized studies on ultrashort laser processing of WBG materials. With this background, this paper reviews the application of ultra-short pulse lasers for the processing of two WBG materials, SiC and GaN. Laser-assisted processing, laser fabrication of microstructures and laser processing of difficult and complex parts are the three main components of ultrashort laser processing of SiC. Ultra-short laser processing of GaN, on the other hand, focuses mainly on laser lift-off and is used less for fabricating microstructures. Physical mechanisms of laser removal of semiconductor materials are summarized. Then, based on the classification of the pulse width, the applications of two types of ultrafast lasers, picosecond and femtosecond, for processing SiC and GaN materials are summarized. Finally, the paper concludes and discusses the existing ultrafast laser processing techniques for SiC and GaN materials and future perspectives.

1. Introduction

Numerous advancements in structure, design, and material qualities have been made to current silicon (Si) technology during the previous decade. Si-based power devices are reaching their performance limits as the current, voltage and temperature requirements of electronic devices continue to increase. In contrast, wide bandgap (WBG) semiconductors are emerging as a possible alternative technology. Silicon carbide (SiC) and gallium nitride (GaN) offer greater voltage breakdown capability, higher switching frequency, similar carrier mobility, larger energy bandgap, and higher thermal conductivity than Si [1]. Fig. 1 compares the properties of three semiconductor materials, Si, SiC and GaN materials, in terms of five aspects: electric field, energy gap, electron velocity, thermal conductivity and melting point, respectively. As a narrow-gap semiconductor material, crystalline silicon has been the backbone of the semiconductor industry [2]. The processing of Si is becoming increasingly sophisticated, and laser processing has unique advantages, especially when it comes to the internal processing of Si materials [3,4]. Focusing the laser on the inside of the silicon can produce permanent changes within the silicon without causing surface damage [5,6]. Better finished products can also be obtained by changing the laser beam [7,8] and combining laser processing with chemical etching [9]. In recent years, more and more researchers have applied these techniques to WBG semiconductor materials. However, WBG semiconductor materials are relatively more difficult to process, and still need a lot of research and exploration. Currently, the research on the

* Corresponding author.
** Corresponding author.
E-mail addresses: peilei@sues.edu.cn (P. Zhang), Tianzhu.Sun@warwick.ac.uk (T. Sun).

https://doi.org/10.1016/j.mssp.2024.108559
Received 20 March 2024; Received in revised form 10 May 2024; Accepted 21 May 2024
Available online 27 May 2024

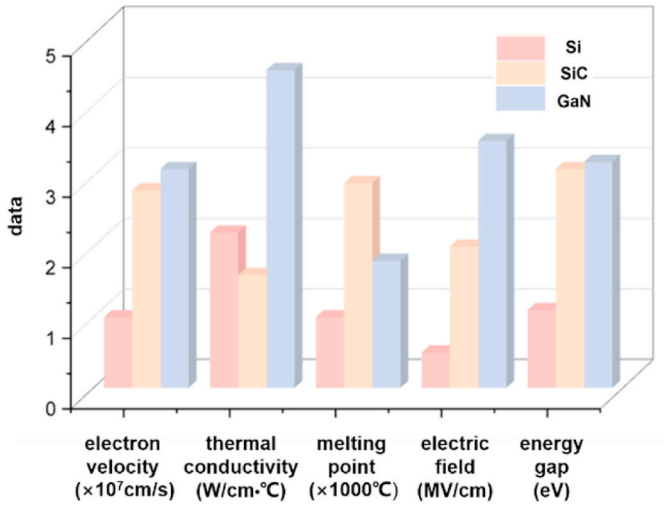

Fig. 1. Comparison of Si, SiC and GaN properties.

processing methods of WBG materials is getting deeper and deeper, and Fig. 2 demonstrates the common SiC and GaN processing methods.

However, several obstacles occur when manufacturing WBG-based semiconductors for a wide range of applications. SiC has a Mohs hardness of up to 9.5 and a bandgap of 3.26 eV [18], and such high hardness and stability make it a difficult material to process. Single-crystal silicon carbide is made of orthotetrahedral silicon-carbon diatomic layers stacked together, in the crystallisation process, the diatomic layers are arranged sequentially as a whole, and the diatomic layers are connected by covalent bonds. According to the different arrangement of stacking cycles of silicon and carbon atom crystal faces, single-crystal silicon carbide can be classified into α-SiC and β-SiC, of which the most common ones among α-SiC are 6H–SiC and 4H–SiC, and β-SiC is also known as 3H–SiC [19]. Among the various types, 4H–SiC is now widely used for its high field strength, high thermal conductivity, and high electron mobility [20], and is widely used in power electronic devices. Commonly used single-crystal silicon carbide processing methods include diamond wire sawing [10], wet etching [11,21] and ultrasonic processing [12]. Compared to these processing techniques, lasers are commonly used to process hard materials [22], and the advantage of

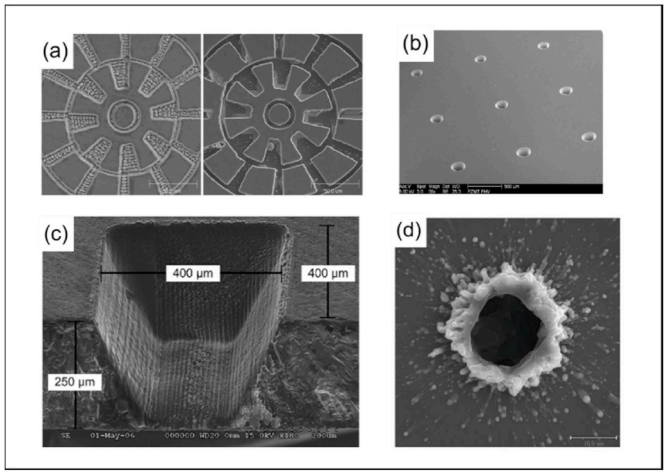

Fig. 3. SiC structures processed with laser: (a) femtosecond laser micromachined rotor [27]; (b) Array of through-vias in a 3C–SiC wafer [28]; (c) ArF laser micromachined trench [29]; (d) femtosecond laser micromachined holes [27].

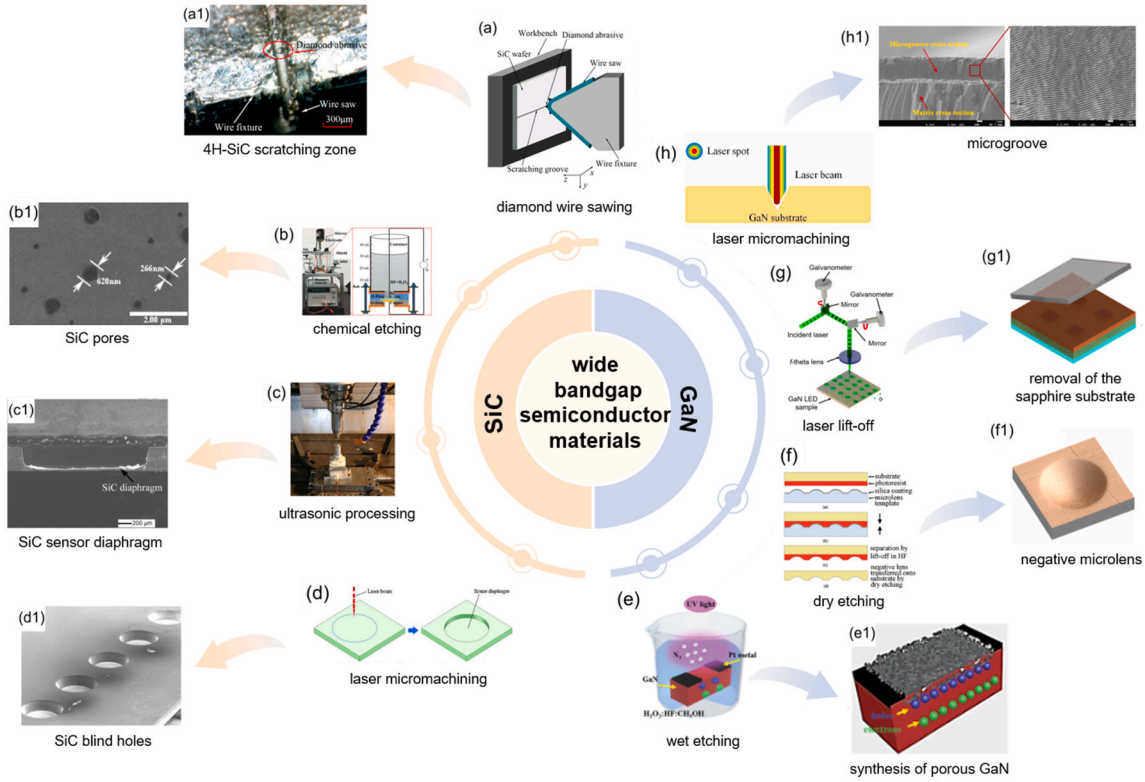

Fig. 2. Processing methods of SiC and GaN: (a) mechanical machining [10]; (b) chemical etching [11]; (c) ultrasonic processing [12]; (d) laser micromachining [13]; (e) wet etching [14]; (f) dry etching [15]; (g) laser lift-off [16]; (h) laser etching [17]; (a1-h1) are the images of (a–h) processing results, respectively.

laser processing is that it allows for higher precision micro and nano processing. Fig. 3 shows some microstructures fabricated using laser processing of SiC. Laser processing injects energy into single-crystal silicon carbide in the form of photons [23], which interact directly with the lattice in the visible [24] and infrared light [25] and have a high absorption rate for it in the ultraviolet laser light [26], thus laser processing allows for the instantaneous removal of the material and high efficiency processing; because of the small focusing spot, the processing parameters are easy to control, so laser processing is easy to achieve precision processing.

As another wide bandgap semiconductor material, GaN has a wide bandgap of 3.4 eV at room temperature and excellent thermal, electrical and optoelectronic properties. GaN also provides a number of advantages, such as smaller size, lower cost, higher efficiency, and faster switching speed. GaN-based devices are currently on the market for radio frequency and laser applications. Since there aren't many high quality, flawless GaN substrates available, GaN epilayers are constructed on foreign substrates like Si, sapphire, and SiC [30–32]. How to strip GaN from the substrate with high efficiency and quality may be a path worth investigating using laser processing technology. Gallium nitride has high hardness and high melting point in physical properties, making it difficult for conventional machining to process micro and nanostructures on the surface of GaN materials. At the same time, GaN is also extremely chemically stable, usually at room temperature GaN material almost does not react with acidic or alkaline solutions [33]. At present, for the preparation of GaN material microstructures are usually used dry etching technology [15], wet etching technology [14], laser processing technology [34] and so on. Dry etching technology is one of the more mature technologies in the processing of GaN materials [35]. As for wet etching technology, GaN materials are extremely stable compounds with strong corrosion resistance [36]. Therefore, wet etching technology is mainly used to etch the defects of GaN materials. At present, it has also become a research hotspot to make use of the special mechanism of the ultrafast laser acting with the material to create a laser-damaged zone on the material surface, followed by dry etching or wet etching. As shown in Fig. 4, the ultrafast laser combined with wet etching technique has eroded high quality inverted hexagonal microstructures on GaN material samples.

This paper highlights recent advances in ultrafast laser micromachining of SiC and GaN, with special emphasis on the different processing focuses of picosecond (ps) and femtosecond (fs) lasers. Section 2 describes the physical mechanism for ultra-short pulse laser processing of semiconductor materials. Section 3 describes the application of ultrafast lasers in processing SiC. Section 4 reviews the applications of ultrafast lasers in processing GaN. Finally, Section 5 describes the current challenges and future prospects.

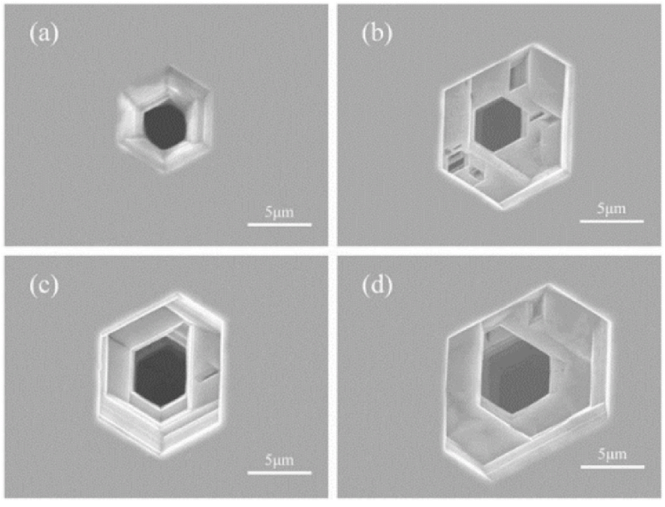

Fig. 4. Microstructural morphologies of GaN after wet etching under different laser energies: (a) 2 mW; (b) 4 mW; (c) 6 mW; (d) 8 mW [37].

2. Physical mechanisms for ultra-short pulse laser processing of semiconductor materials

In this chapter, we will address the important theoretical foundations for understanding the experimental setup, findings and discussions in papers. The characteristics of ultra-short pulse laser and their physical mechanisms in processing semiconductor materials will be presented.

2.1. Characteristics of ultra-short laser

Picosecond and femtosecond lasers both belong to the category of ultrafast lasers, they have extremely short pulse durations that enable the laser energy to be efficiently delivered into the material prior to thermal diffusion. Compared to long-pulse lasers, ultrafast lasers are unique in their multi-photon ionization and reduction of electron-to-lattice energy transfer, resulting in negligible thermal damage, so they can be referred to as "cold ablation," as illustrated in Fig. 5. Srinivasan et al. [38] and Küper et al. [39] first reported using ultra-short pulse lasers for material processing in 1987. And the ablation threshold of ultra-short laser is significantly lower than the ablation threshold of ns laser. At the conclusion of the laser pulse, electron-lattice scattering allows for efficient energy transfer from electrons to the lattice [40]. The usual electron-phonon coupling duration of 100 fs is substantially shorter than the thermal conduction heat-transfer period. As a result, heat diffusion to the laser-irradiated surrounding region is relatively restricted [41], making high-resolution ultrafast laser processing particularly appealing. Ultrafast lasers allow high-precision micro- and nanofabrication of a wide range of materials, such as metallic glasses [42], biological tissues [43], semiconductors [44] and insulators [45]. Ideally, rapid excitation occurs only within the focus point. Thermal diffusion, on the other hand, cannot be ignored for a laser pulse with a length of a few nanoseconds or more.

2.2. Physical mechanisms of ultra-short laser ablation

In contrast to other processing methods, ultra-short pulse laser irradiation is able to bring the material into a non-equilibrium state and trigger structural transitions, resulting in complex multi-scale surface morphology, unusual sub-stable phases and microstructures. Fig. 6 illustrates the interleaving process triggered by ultra-short laser pulses in a semiconductor material. In semiconductors, non-thermal phase transitions may be induced by laser radiation leading to transient modifications of interatomic bonds [46,47]. In metals, due to the presence of

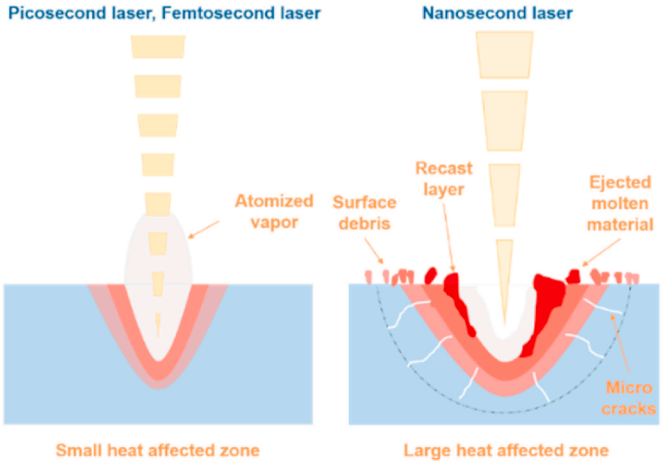

Fig. 5. Schematic of ablation for nanosecond and ultra-short lasers.

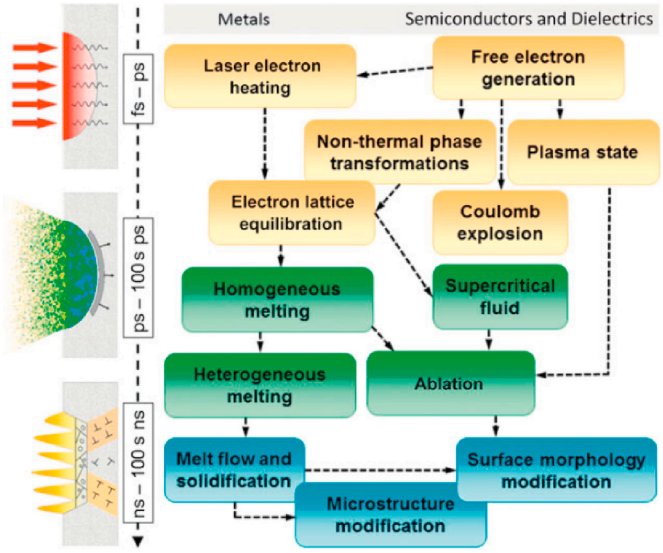

Fig. 6. Pulsed laser-material interaction processes [56].

conduction band electrons, electrons can absorb laser energy directly upon collision with the nucleus. In semiconductors and dielectrics, electrons must be excited across the band gap before they can directly absorb photons [48]. Simultaneously, excited electrons in semiconductors can easily absorb laser energy, which could lead to the material entering a plasma state or possibly causing a Coulomb explosion owing to electron emission [49]. For wide bandgap materials, due to their large bandgap widths, the main mechanisms for the generation of free electrons from photons with energies below the bandgap are multiphoton and avalanche ionization, which are highly nonlinear processes [50]. The energy transfer from the electrons to the lattice vibrations causes rapid heating, which results in uniform melting of the material or even the formation of supercritical fluids [51]. Extreme temperature and pressure conditions brought on by the quick deposition of laser energy may result in the formation of unusual metastable phases [52] and complex surface morphology [53] from photomechanical spallation [54] or the explosive breakdown of superheated material into a mixture of vapor and droplets [55].

The ultra-short laser pulse's energy mostly bonds to the material's electrons when it is exposed to radiation. Electrons in semiconductors cannot absorb photons directly; instead, they must be stimulated over the bandgap [57]. In materials having a bandgap, electronic stimulation has the potential to significantly alter the interatomic bonding and cause ultrafast phase transitions, such as melting [46] and solid-solid phase transformations [47]. Since these phenomena occur on sub-picosecond time scales, are immediately triggered by the laser excitation, and do not require lattice heating or electron-phonon equilibration, they are called "non-thermal."

The removal of material by direct absorption of laser energy is referred to as laser ablation. When laser beam interacts with materials, the rapid energy deposition rate of ultrashort laser pulses may generate compressive stresses. When the time of the laser heating is shorter than the time required for the mechanical relaxation (expansion) of the heated volume, the laser-generated stresses are particularly high in the regime of stress confinement [54,58]. Compression stresses interact with the surface of the irradiated specimen and produce a tensile wave that is sufficiently strong to induce the formation of subsurface voids, as shown in Fig. 7. Development of voids and seepage may lead to top separation and ejection of the target [56]. The growth and infiltration of the cavity might cause the upper layer to separate and eject. Like the term "spallation", it is normally applied to the phenomenon that the shock waves reflect on the back surface of a specimen, but it is usually called a photomechanical spallation.

Thicker layers and/or multiple droplets are separated and ejected from the target as a result of further increases in laser energy density above the spallation threshold. With high enough laser energy density, this causes a transition to an alternate ablation regime known as "explosive boiling" or "phase explosion". Under this regime, the irradiated target's melted surface region overheats above the liquid phase's thermodynamic stability limit [55], causing the overheated molten material to rapidly break down into a mixture of liquid droplets and vapor. A sharp increase in the number of vapor-phase atoms in the ejected plume indicates the shift from photomechanical spallation to phase explosion [60], reflecting the different physical principles behind the material ejection in these two regimes. When longer laser pulses are used for ablation, there is no stress confinement, so explosive boiling is the process that directly moves from the regime of surface melting and evaporation to the phase explosion without activating spallation [55]. Since the spatial variation of laser intensity in a laser beam usually has a Gaussian profile, photomechanical scattering and phase explosion may coexist and together contribute to the material ejection induced by the same laser pulse, as shown in Fig. 8.

For ultrafast laser pulses, the Coulomb explosion (CE), a material removal mechanism, dominates at low laser intensities near the ablation threshold [61]. Laser impacts cause a large number of electrons to be emitted from the target, leaving positive holes in the near-surface region. In semiconductors, the time for a large number of electrons to fill these holes is about picoseconds or even longer [62]. As a result, the neighboring region of the surface is positively charged for a considerable period of time. This charged region may become electrostatically unstable, so that with a sufficiently high density of holes, the surface breaks up by the emission of positive particles, which are accelerated in the residual field. This electrostatic repulsion is known as a Coulomb explosion [63]. The clean, undamaged surface [64] that is left behind when CE occurs makes this ablation mode very appealing for nanoscale

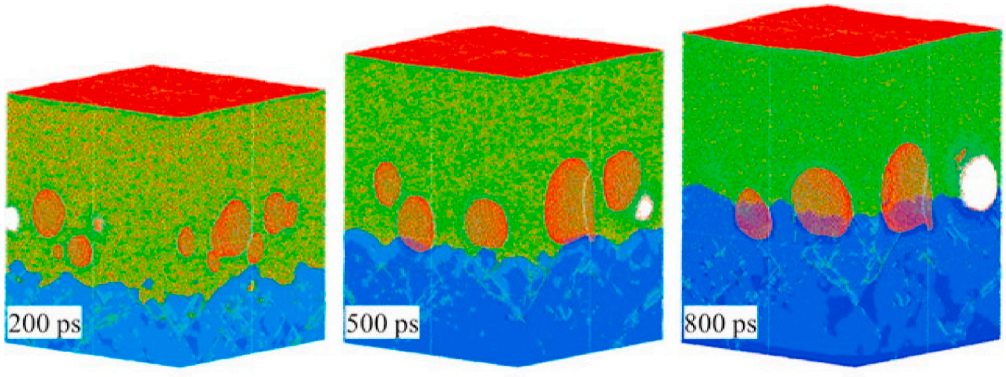

Fig. 7. Snapshots of atomic configurations produced in a 100 fs laser irradiation simulation [59].

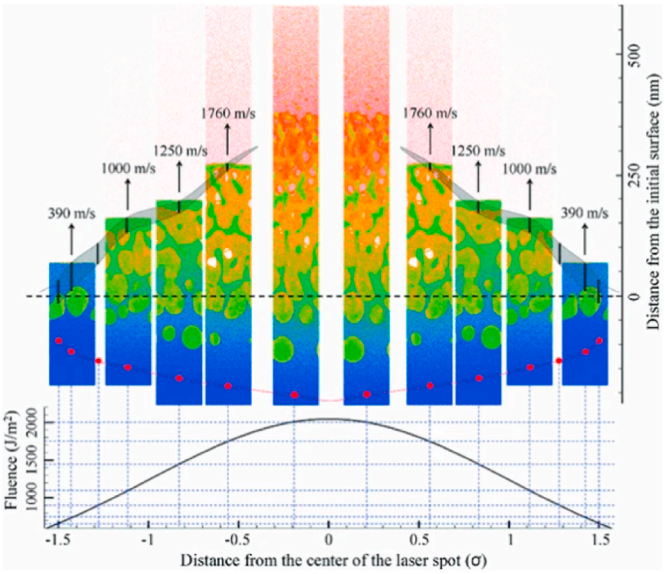

Fig. 8. Overall visual image of an aluminium target melting under 100 fs laser irradiation, creating subsurface voids and material ejection [60].

material processing. There are hints that semiconductors at laser energy density over the plasma generation threshold may experience CE [62]. Under such conditions, ions from CE account for only a small fraction of the ablation product [65].

In wide bandgap materials, light can only be absorbed when the photon energy is higher than the bandgap, thus promoting electrons from the valence band to the conduction band—this is the linear absorption; when the single photon energy is lower than the bandgap, the main mechanisms by which photons produce free electrons are photoionization and avalanche ionization, the first process can be divided into two different cases, tunneling and multiphoton ionization—this is the process of nonlinear absorption [66]. It is through nonlinear absorption processes that laser absorption in SiC and GaN is achieved [67]. With the deeper understanding of laser-material interactions, the smallest feature sizes achievable by laser processing techniques have been gradually reduced from micro to nanometric [68]. Most of the current researchers use the dual-temperature model to simulate ultrashort-pulse laser ablation [69]. Further improvement of precision and surface quality is a great challenge, and the study of material processing mechanisms is of great significance for micro- and nano-fabrication.

3. Ultra-short laser processing of silicon carbide

Having understood the physical process of laser-material interaction, we need to learn how this physical process is applied. Numerous studies have shown that this complex interaction is often used to silicon carbide micromachining. That is, by changing the laser parameters, the medium in the process and other conditions, SiC is directly laser micromachined or processed using laser-assisted other processes. The size of the processed microstructures ranges from micrometers to nanometers, including cuts, through holes, thin films, surface structures and so on. Therefore, this chapter discusses the use of ultrafast laser processing of common structures in silicon carbide materials.

3.1. Picosecond laser processing

In the 1960s, researchers created mode-locking and generated picosecond lasers [70]. Since then, picoseconds have played a significant role in modern processing technology, especially in processing high hardness materials. Picosecond pulsed laser have the advantages of low thermal effects, small heat-affected zones, precise control of machining geometry, high efficiency and good repeatability. Picosecond lasers are a powerful technology in manufacturing, especially when the desired feature size is micron and submicron. With the right laser parameters, picosecond laser processing can achieve the same level of accuracy as femtosecond laser [71]. Therefore, it has a great potential for research in the field of etching silicon carbide.

3.1.1. Laser cutting

In order to satisfy the requirements of practical applications, silicon carbide wafers are always required to be cut into various shapes and sizes. The main methods currently used in industry to cut silicon carbide wafers include mortar wire cutting, diamond wire saw cutting and laser cutting. Silicon carbide is a material with a Mohs hardness as high as 9 [72] and a low fracture toughness [73], requiring the use of diamond grinding wheels to cut it [74]. However, even cutting with diamond wheels still has drawbacks, so many research groups have applied laser technology to SiC processing, Fig. 9 shows the cut surfaces obtained by mechanically cutting SiC and three different SiC laser cutting techniques. Compared with mechanical cutting, laser cutting of SiC can effectively reduce mechanical stress, and the heating zone is smaller, the material loss is lower, and the surface quality is higher. In addition, laser cutting is much faster than diamond cutting. The researchers found that the laser pulse width largely determines the cut quality of SiC wafers. Cutting silicon carbide with nanosecond lasers always results in a large heat-affected zone (HAZ) and unavoidable thermal damage [28]. Cutting silicon carbide with ultra-short pulse lasers significantly reduces the HAZ and achieves better quality [75,76]. However, there are some problems associated with direct cutting of SiC using picosecond lasers, such as the presence of contaminants [77], unstraightened cutting slits [78], and noticeable consumables. SiC wafers are expensive [79], and there is a need to minimise material loss during the cutting process. To improve the cutting quality of SiC wafers, laser stealth dicing (SD) has been proposed for the cutting of semiconductor wafers. The laser stealth dicing technique was proposed by Ohmura et al. [80] in 2006, whereby a laser is focused inside the silicon wafer to form a modified layer, which acts as a guide for crack initiation sites and separation, and then destroys the wafer by applying an external force along the cut line. Stealth scribing thus enables, zero kerf, zero taper and no surface sputtering. In addition, Kumagai et al. [81] used a modification layer on a 50-μm-thick Si chip with SD, and then the wafer was divided by tape expanding. In the course of cutting, there is no splashing, cracking, or winding of the parting line. There was no surface sputtering, chipping, or meandering of the parting line during the cutting process. The tape separation method used in the study was innovative. Since the introduction of invisible cutting, many researchers have studied it in the hope of perfecting the technology and putting it into production soon. Kim et al. [82] investigated the effect of pulse width on the modified structures by stealth cutting 420 μm-thick 4H–SiC wafers using a 780 nm, 1 kHz laser with a single pulse energy of 10 μJ and a selectable pulse width from 220 fs to 6 ps. It is found that when the laser scanning speed is 2 mm/s and the pulse width is more than 750 fs, the modified structure starts to appear inside the wafer, and as the pulse width increases from 750 fs to 6 ps, the modified structure gradually becomes longer and appears to be segmented, as shown in Fig. 10(a). The researchers also investigated the internal structural changes in the double-pulse case, as shown in Fig. 10 (b). The researchers speculated that in the case of double-pulse femtoseconds, the structure induced by the first pulse was able to significantly absorb the energy of the second pulse, thus preventing the extension with laser propagation.

In addition to the exploration of suitable laser parameters, the researchers also propose new solutions by changing the laser processing steps. Zhang et al. [84] used a novel dual laser beam asynchronous dicing method to cut 200 μm-thickness-SiC. Firstly, a 750 fs, 532 nm laser beam with a repetition frequency of 20–200 kHz and a maximum output power of 5 W was used to generate the modified layer inside the wafer at a scanning speed of 3 mm/s; then a continuous laser beam of

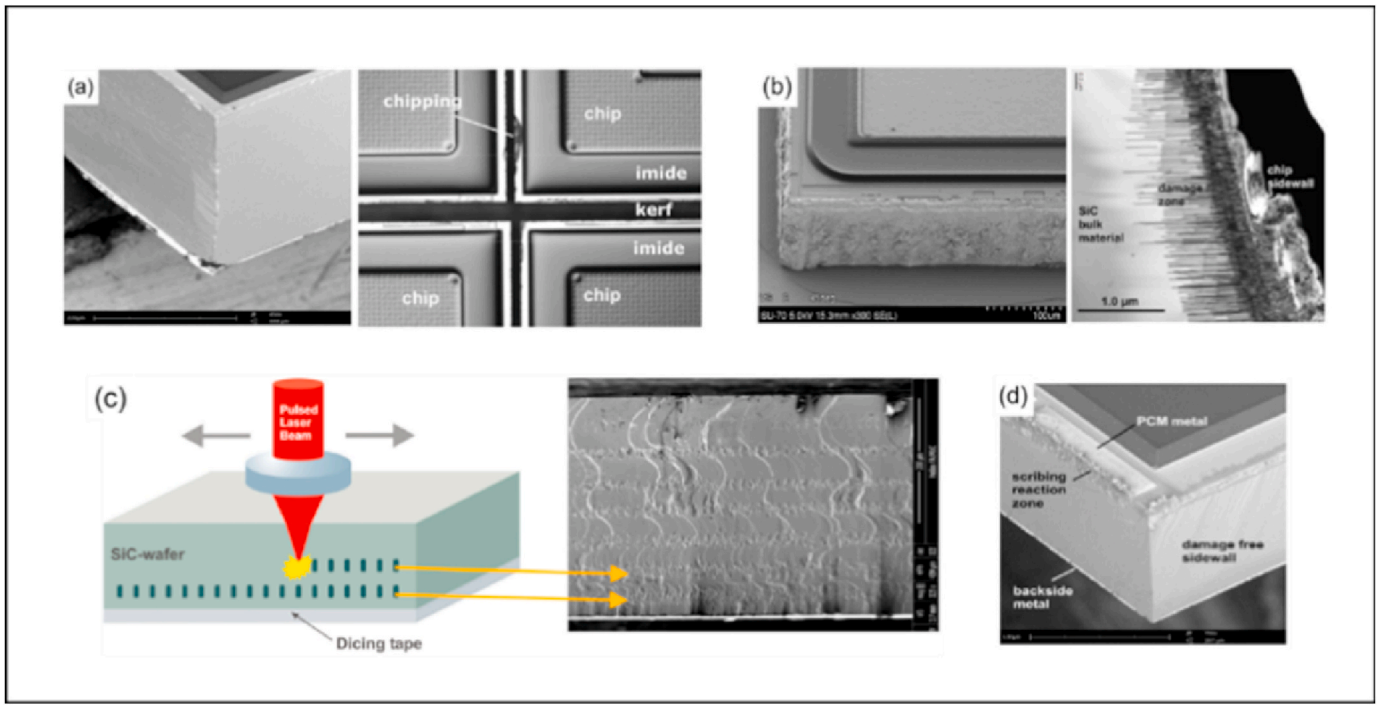

Fig. 9. SiC cutting techniques: (a) Mechanical cutting; (b) Laser ablation cutting; (c) Stealth cutting; (d) Thermal laser separation [83].

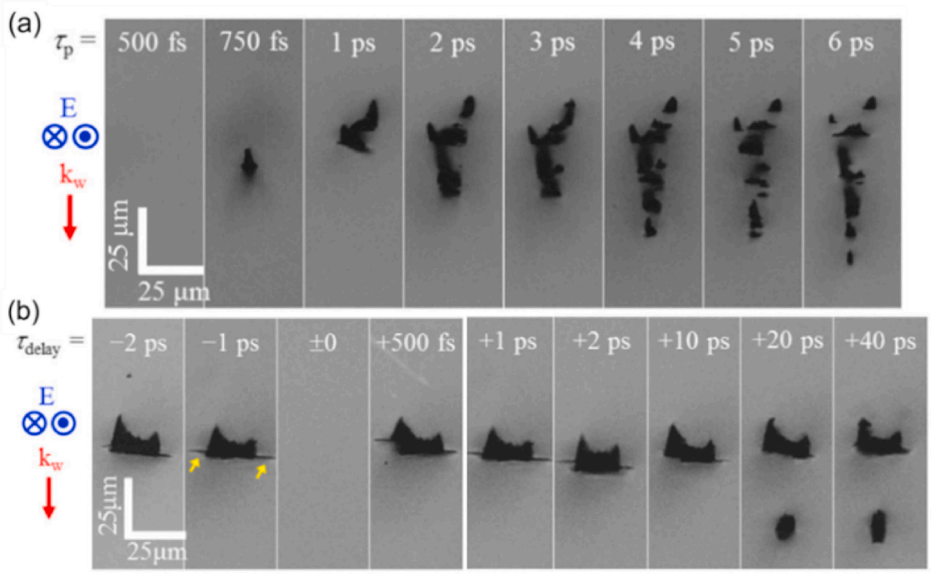

Fig. 10. Cross section of ultra-short pulse laser-induced internal structure of 4H–SiC: (a) single-pulse laser; (b) double-pulse laser [82].

1040 nm with an output power of 8 W was used to heat up the modified layer. The thermal stress generated by the laser beam induces cracks in the modified layer to expand perpendicular to the wafer surface at a scanning speed of 1000 mm/s. The laser beam is used to generate a crack in the modified layer. Fig. 11 shows the results of cutting the SiC wafer with a thickness of 200 μm using dual laser beam asynchronous dicing method. Wang et al. [85] used femtosecond laser and picosecond laser to study the structural evolution and defect formation mechanism during 4H–SiC stealth cutting, and found that due to the minimization of thermal effects, femtosecond laser stealth cutting has a higher processing accuracy, and the processing efficiency of picosecond laser processing is higher picosecond laser efficiency under the same laser energy density. In the above laser stealth cutting SiC wafer experiments, the femtosecond laser scanning speed is slow (<5 mm/s) because the femtosecond pulse induces small modified structures, and the scanning speed needs to be reduced to make the neighboring modified structures closer to ensure the wafer lobing effect. Unlike femtosecond pulses, picoseconds (>20 ps) induce avalanche ionization of the wafer [50]. Under the continuous action of the pulse, the electrons have enough time to transfer the absorbed energy into the lattice, resulting in melting or even rupture of the lattice, which increases the modification range of the pulse. Ohmura et al. [80] apply nanosecond pulses to stealth-cutting of silicon wafers with low thermal conductivity, while when it stealth-cutting of SiC wafers with higher thermal conductivity than copper, the nanosecond pulse modifies the wafer for too long, which has a strong thermal effect on the wafer and It is easy to damage the wafers.

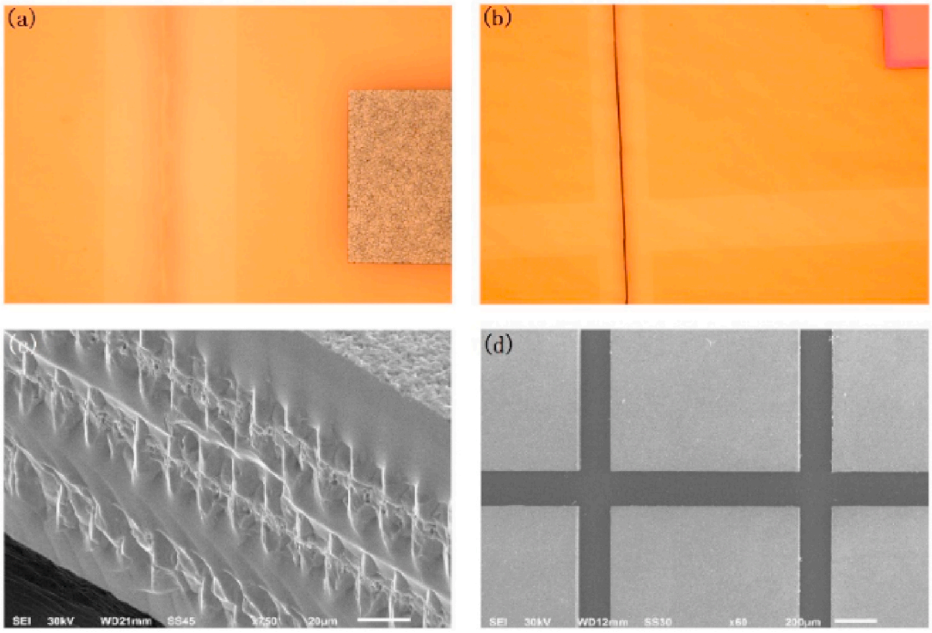

Fig. 11. The results of cutting 200 μm SiC: (a) The surface after the stealth dicing; (b) The thermal crack from the continuous laser; (c) The cutting profile and; (d) The final separation after the expanding process [84].

Using picosecond pulses with pulse widths between femtoseconds and nanoseconds to stealth cut SiC wafers, balancing the modification range of the pulses and the thermal impact, it may be possible to obtain high-quality, high-speed stealth cutting results.

Yang et al. [86] successfully separated SiC wafers with high-quality cuts by the precision layered stealth dicing method using ultrafast picosecond lasers, and obtained a cross sections with roughness of about 1 μm. It is pointed out that the anisotropy of SiC wafers leads to the varying quality of precision layered stealth dicing cross sections, with the roughness of crystalline surface {10-10} being 20 % lower than that of crystalline surface {11–20}, which provides a direction for the study of wafer dicing of SiC in terms of crystal orientation. Since single-crystal SiC wafers are anisotropic, the cutting effect on different faces is naturally different. Silicon carbide has two unequal faces, the Si-face (0001), and the C-face (000 $\bar{1}$), as shown in Fig. 12. Wen et al. [87] internally modified 4H–SiC by picosecond laser and subsequently cleaved by three-point bending test. It was found that the 4H–SiC samples treated along the [11 $\bar{2}$ 0] crystal orientation were easier to be cut and the C-face of 4H–SiC was more rigid and the Si-face was more elastic and ductile. Fig. 13 shows the edge chipping of SiC samples along different crystal orientations. It can be clearly seen that the edge chipping width of SiC samples cut along the [11 $\bar{2}$ 0] crystallographic direction is smaller and the kerf is neater compared to the [1$\bar{1}$ 00] crystallographic direction.

3.1.2. Laser drilling

When drilling silicon carbide, the pulse energy and laser pulse width

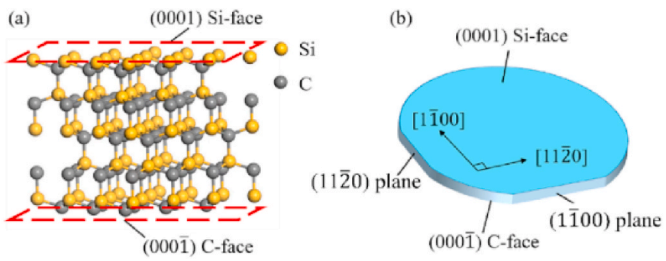

Fig. 12. Crystal structure of 4H–SiC (a) and crystal orientation of wafers (b) [87].

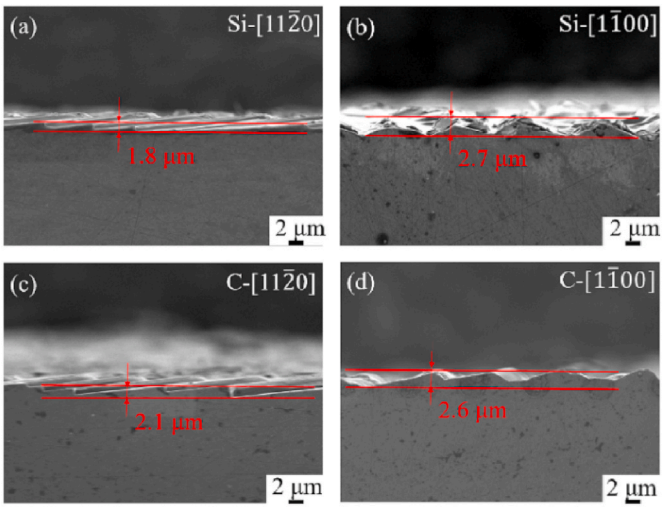

Fig. 13. Top-view SEM images of edges of silicon carbide samples cut along different orientations [87].

have a great influence on the drilling results. In order to investigate the damage induced by stress waves during ultra-short laser drilling, Hattori et al. [88] used pump probe imaging and high speed camera to investigate the damage caused by stress waves during ultra-short laser drilling. The high speed dynamical course of the propagation of stress waves and the formation of cracks in ultra-fast laser drilling was observed by means of the pump probe imaging and high speed video camera. As illustrated in Fig. 14 (a), the greater the impulse power, the bigger the aperture size, the stronger the stress wave and the bigger the damage zone. Fig. 14(b) shows the images for different pulse widths at 50 μJ pulse energy. The results show that the damage and stress waves at 180 fs are significantly smaller than those at 1 ps. This is due to the fact that the excited electron density is easily close to the critical value, which leads to total internal reflection and lower penetration depth. Thermal damage, small stress waves, and low drilling speeds were observed at the orifice at 10 ps due to the low laser intensity, which makes multiphoton

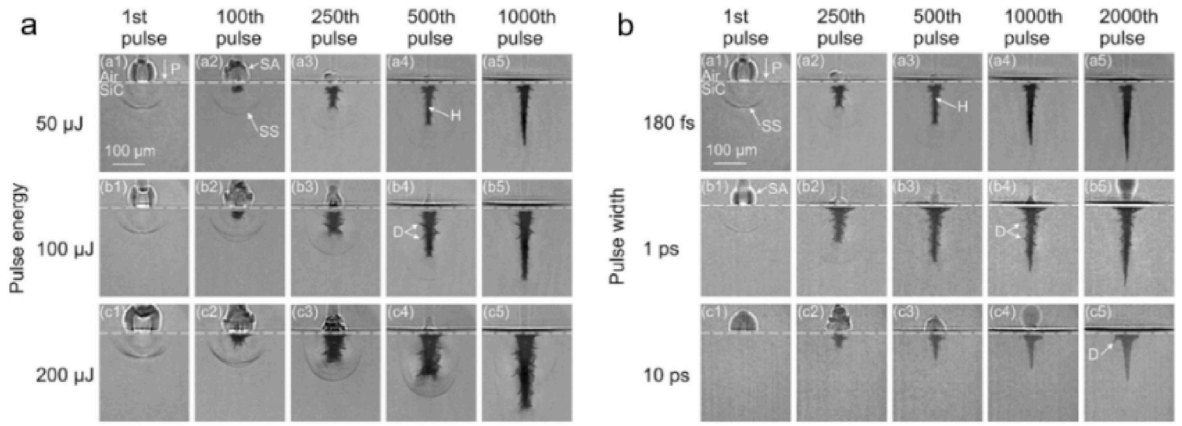

Fig. 14. Ultrafast laser drilling of SiC: (a) Shadowgraphs after 6 ns of different pulse energies at 180 fs; (b) Shadowgraphs for 6 ns after a different number of pulses and pulse widths at 50 μJ [89].

absorption unlikely [89]. Hattori et al. subsequently concluded that tensile stress is the stress that leads to fracture damage. The damaging mechanism caused by laser drilling should be researched further in order to improve damage control methods and expand the industrial application of SiC [90].

3.1.3. Other laser processing

Rapid non-thermal ablation of pressure sensor diaphragms with a picosecond laser is reported by Pal Molian et al. [77]. When the pulse repetition frequency is less than 250 kHz there is a non-thermal ablation mode and the grooves and holes obtained have clean and smooth edges; when the pulse repeat rate is raised to 500 kHz, carbon material and re-cast layers are present in the processed region, which may be attributable to atmospheric plasma interaction with nanoparticles. Fig. 15 shows the grooves obtained by processing SiC using a 50 kHz picosecond laser, with smooth sidewalls, sharp edges, and debris accumulating at the ends of the grooves, which could not be removed with cleaning gas. The bottom of the grooves was extremely smooth without any traces of melting, micro-cracks or other heat damage. The bottom area of the 3C–SiC, as opposed to the nanosecond pulsed excimer laser micromachining, was wavy or corrugated [28]. When a 500 kHz laser was used to process above the material surface, a black compound appeared in the ablation zone; this was determined to be carbonaceous material due to thermal decomposition of the SiC.

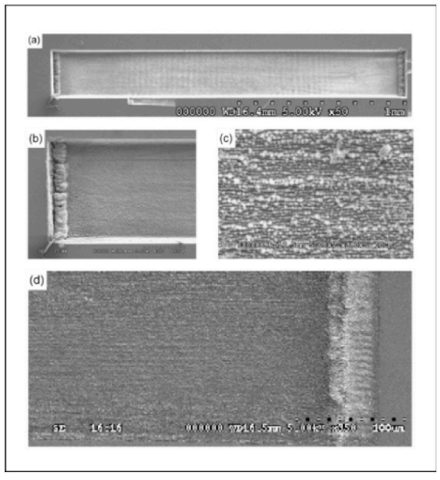

Fig. 15. Laser-machined 4H–SiC grooves: (a) 4H–SiC ablated at a laser frequency of 50 kHz; (b) Enlarged view of the left end of Fig.15(a); (c) Bottom of SiC grooves; (d) Decomposed carbon products formed above the surface of the material when the laser is focused at a focal point of 500 kHz [77].

Xu et al. [91] used a picosecond of 355 nm with a processing frequency of 200 kHz to process microstructures on SiC, and found that picosecond laser processing can precisely control the morphology of the microstructures processed on SiC, and that more fine microstructures can be obtained by suitable processing parameters. And the principle of ablation effect of picosecond laser on the surface of SiC was investigated, and it was found that the laser processing effect was mainly ablation, supplemented by remelting. During laser processing, the silicon carbide absorbs the laser energy and decomposes and sublimates during the ablation process. The experimental use of picosecond laser energy density in the spot according to the Gaussian distribution, when the laser energy from the center of the spot to the outside, the spot shape will maintain the original laser density distribution. At the same time, in the laser processing process, the silicon carbide exists an ablation threshold, only when the energy density is higher than the ablation threshold, the silicon carbide will be ablated, which leads to an incomplete Gaussian distribution of the shape of the laser processed grooves in an inverted triangle.

3.2. Femtosecond laser processing

The invention of collision pulse mode locking technology and the advent of femtosecond lasers date back to the 1980s [92]. For more than 20 years, there have been many reports on femtosecond lasers in processing of silicon carbide, which can be summarized in three main areas. First, the use of femtosecond laser-assisted processing. Second, the use of femtosecond lasers for the fabrication of micrometre or nanostructures, such as through-holes, thin films and surface structures. Third, femtosecond laser processing of difficult and complex parts, such as cutting. This section will also discuss in this order.

3.2.1. Laser-assisted processing

SiC has a very high physicochemical stability and is often processed inefficiently, but it has been found that the surface or internal structure can be modified by laser radiation to make processing easier [93]. Brewer et al. [94] used a 160 fs, 780 nm femtosecond laser to treat SiC and found that the threshold and nonlinear properties of SiC were disrupted, demonstrating that femtosecond laser irradiation affects SiC in some way. Vanthanh et al. [95] used a 120 fs, 800 nm femtosecond laser to treat 6H–SiC and found that a mixture of hydrofluoric acid (HF) and nitric acid (HNO_3), which do not react with 6H–SiC at ambient temperature, could etch a region of laser irradiation in order to form through holes. Fig. 16 shows the laser-induced structural changes and the morphology of the chemical etching-induced silicon carbide grooves. This indicates that 6H–SiC exhibits more active chemical properties after femtosecond laser irradiation and can be more easily processed and fabricated. Gao et al. [96] et al. took advantage of such

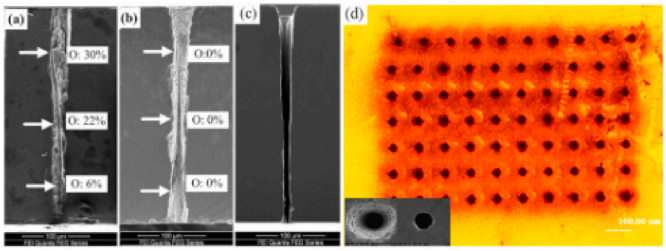

Fig. 16. SEM morphology of SiC through hole: (a) Laser-affected zone (LAZ); (b) Structure after etching; (c) Cross-section of the microgroove; (d) Through-hole array, insets showing the entrance and end portions of the holes, respectively [95].

properties by using femtosecond laser irradiation at of 800 nm, 150 fs, and 1 kHz to form a periodic line corresponding to laser-induced structural change (LISC), then removing the periodic line with a mixture of HF and HNO_3. The SiC material in the LISC region was then removed with a mixture of HF and HNO_3 to form a grating groove. Grating grooves with a large aspect ratio of about 25 were obtained. Meng et al. [97] utilised a 520 nm, 300 fs laser to scan a 4H–SiC surface to produce a modified surface layer with a periodic micro/-nanostructure. As shown in Fig. 17, the 4H–SiC surface that was scanned by a fs laser was characterized by a low-space-frequency ablative track related to a scanning path, and a high-space-frequency fluctuation pattern was observed. The laser-induced periodic surface structure of SiC and the machinability of its modified layer were investigated, and the results show that femtosecond laser surface modification can shorten the extrusion stage in the 4H–SiC machining process, and effectively improve the material removal efficiency and machinability.

Etching is a key process for SiC manufacturing [98]. Typical SiC etching processes are (1) mechanical machining, (2) molten salt corrosion, (3) wet etching such as photo-electrochemical corrosion [99] or electrochemical corrosion [100,101], (4) dry etching such as inductively coupled plasma etching (ICP) and reactive ion etching (RIE) [13]. Among these etching methods, dry etching is one of the most commonly used techniques for etching silicon carbide, which is mature and widely used. Comparatively speaking, wet etching technology has the advantages of fast speed and simple process in realizing the processing of micro and nanostructures, but wet etching will etch all directions uniformly, which leads to the loss in the transverse direction, and it is also prone to environmental pollution. Huang et al. [102] treated 6H–SiC substrates using a femtosecond laser with 120 fs, 800 nm and a repetition frequency of 1 kHz to produce an irradiated region. The results show that the femtosecond laser-induced top SiO_2 and rough surface increased the rate of ICP etching. As the EDS analysis in Fig. 18 shows, O elements are found only in the irradiated region. The reason for this may be that during laser irradiation and modification, the SiC lattice is disrupted and the O elements in the air combine with the Si elements to form silicon oxide (SiO_2), which accumulates in the irradiated area. SiO_2 is easier to process than SiC, so after laser irradiation, the maximum increase in ICP etching rate was 117.18 % compared to the untreated ones. Also choosing to use femtosecond laser modification were Xie et al. [103] who irradiated SiC substrates with a femtosecond laser at 290 fs, 515 nm, maximum output power of 8 W and maximum repetition frequency of 600 kHz. The results showed that Si–O compounds were formed on the laser-irradiated SiC surface, which made the subsequent chemical mechanical polishing (CMP) process 2–3 times more efficient than that on the unirradiated surface due to its lower hardness. In addition, the selection of appropriate femtosecond laser parameters to irradiate the SiC substrate to form a uniform periodic corrugated structure will also help to improve the surface flatness.

3.2.2. *Laser fabrication of micro/nanostructures*

The fabrication of through-holes in SiC materials facilitates heat dissipation in next-generation microelectromechanical systems, and the use of laser machining improves machining efficiency and accuracy due to the difficult machinability of SiC. Femtosecond lasers are powerful tools for processing three-dimensional micro/nanofabrication [104].

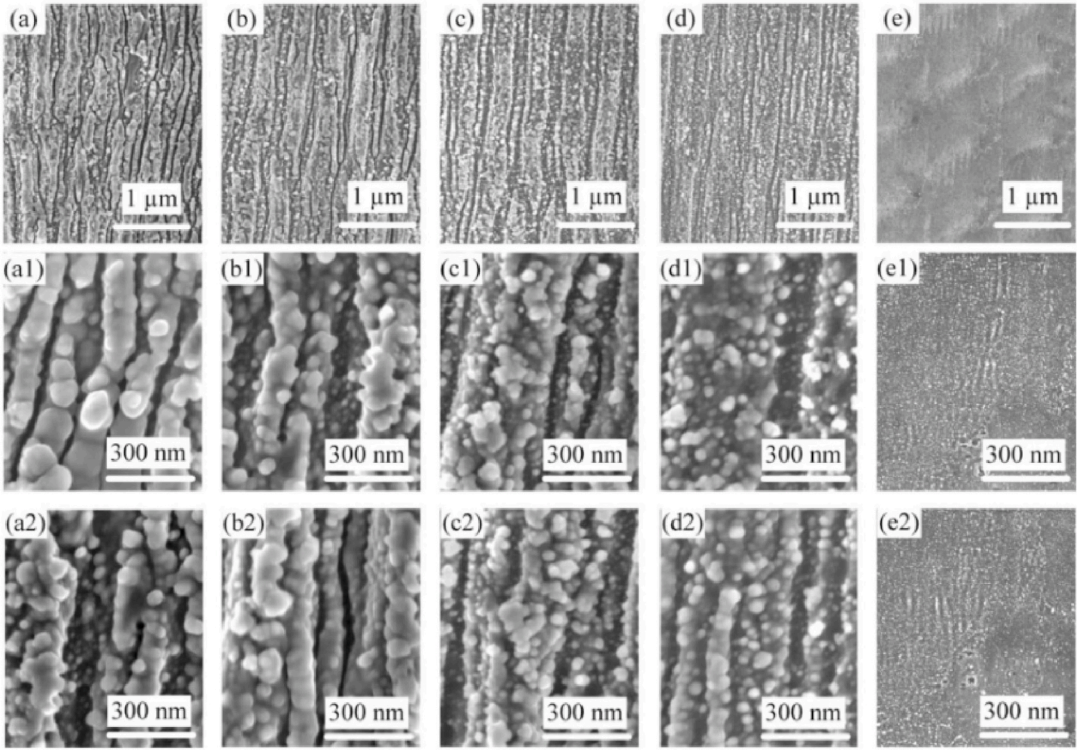

Fig. 17. 4H–SiC surface after femtosecond laser scanning: (a–e) Ablation structures in the modified layer region, where (a1-e1),(a2-e2) are partially enlarged images of the modified layer regions (a–e) [97].

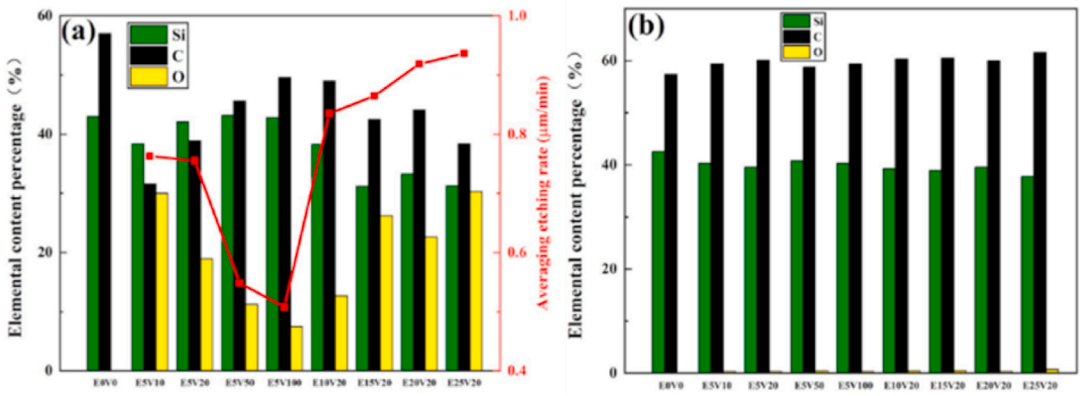

Fig. 18. (a) Relative elemental content of unirradiated and irradiated areas before ICP etching and its relation to the average ICP etch rate for all irradiated areas; (b) Relative elemental content of unirradiated and irradiated areas after ICP etching [102].

Farsari et al. [105] used a 200 fs,1030 nm laser to drill holes in 400 μm thick 3C–SiC. As illustrated in Fig. 19, the inlet diameter of the micro-aperture is about 20 μm, and the outlet diameter is about 5 μm. Erosion fragments, cracks, etc., were observed in the inlet, and a reforging layer was observed in the interior of the cavity. Li et al. [106] further improved the femtosecond laser drilling of silicon carbide using ethanol. The study utilised an 30 fs, 800 nm, 1 kHz laser to scan along a circular path for 3 s at 50 μm/s. Before the laser was incidenced, an alcohol drop was placed on the wafer. The ablation debris was then removed using flow and volatilization. Fig. 20 shows deeper and cleaner holes than those machined in air with the same parameters. However, this method is difficult to control and the alcohol is flammable and volatile, making it dangerous to operate. Khuat et al. [95] used a 120 fs, 800 nm femtosecond laser to prepare through holes in 6H–SiC. and ultrasonically cleaned by a mixture of HF and HNO_3 solution, which effectively removed the ablation debris and recast layer, but the cross-sectional morphology was poor, cracks still existed, and the taper was large. Wang et al. [107] placed 350 μm thick 4H–SiC wafers under a 500 μm water film and impact drilled the holes using a 240 fs, 515 nm, 50 kHz, 60 μJ laser. The holes were more round and have no cracks, material spalling or recast layers on the surface compared to drilling in air. High-quality through-hole arrays with an aspect ratio of 10 were drilled on 4H–SiC with optimal water film thickness, as shown in Fig. 21. This indicates that the underwater treatment effectively improved the quality of the holes. On this basis, Wang's group [108] also used both the protective layer and water to assist the drilling process in femtosecond laser drilling with the same parameters. It is found that proper protection and proper thickness can be used to enhance the inlet shape. But the outward appearance is bad, and there are reamed layers and ablative fragments in the interior of the cavity, so it is necessary to get rid of them with ultrasound and chemical etching.

Femtosecond lasers theoretically enable cold machining of microstructures without defects such as cracks, recast layers, and heat affected zones. Dong et al. [110]. used a 120 fs, 800 nm, 1 mJ femtosecond laser to prepare circular diaphragms on 250 μm thick 4H–SiC wafers by trepanning mode and via holes by percussion drilling mode. Superior thickness, high-aspect ratio, space resolution and thin film were obtained by 'non-thermal' ablation mechanisms. Zehetner et al. [111,112]. prepared circular film arrays with diameters of 1000~3000 μm and thicknesses of 75 μm on 350 μm thick 4H–SiC wafers by femtosecond laser ablation at 350 fs, 520 nm, and 200 kHz. The paper demonstrates that ultra-short pulse laser ablation can fabricate diaphragms with thicknesses in excess of 20 μm in a wide range of difficult-to-machine materials at speeds up to five times faster than ion etching. But there is no explicit information about the processing quality of fs-laser, including surface roughness, edge quality, side slope, etc., which are very important to measuring precision and intensity of the finished transducer. In order to figure out the actual processing quality of femtosecond laser in the fabrication of sensitive diaphragms for high-temperature pressure sensors in silicon carbide, Zhao et al. [13]. reported that blind holes were prepared by femtosecond laser microfabrication at 1064 nm on 350 μm-thick 4H–SiC wafers for obtaining sensitive diaphragms of pressure sensors with a thickness of 80 μm. By testing various parameters of the processed structures, it was concluded that femtosecond laser micromachining exhibited high machining accuracy, good sidewall steepness and smooth machined surfaces during deep etching of silicon carbide. Fig. 22 shows the sidewall morphology of the blind aperture with a rough bottom of the sidewall and grooves on the edges of the sensitive diaphragm, which is due to over-etching. Wang et al. [113]. used a 200 fs, 1030 nm laser to drill blind micro holes in a circular sensor diaphragm. The precision of the machining depth of the blind hole is not higher than 2 % and the surface roughness is 153 nm. Zhao et al. [114]. used a 300 fs, 1035 nm, 100 kHz laser to prepare 4H–SiC sensors by releasing a 600 μm radius and 60 μm thickness bulk SiC film directly from a 4H–SiC wafer. The study demonstrates the feasibility of femtosecond laser technology for rapid prototyping of bulk SiC pressure sensors applied in extreme temperature environments.

It has been demonstrated in many studies that laser irradiation of

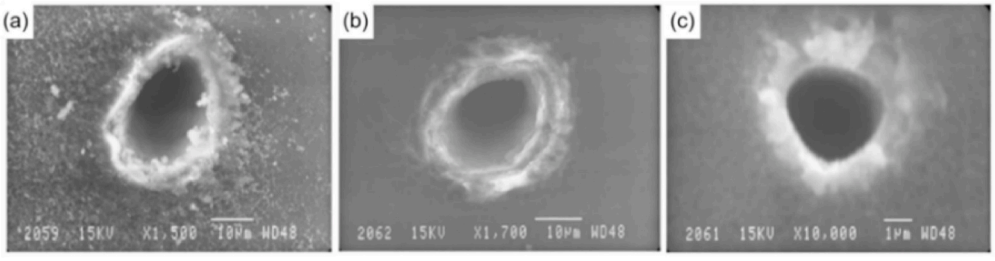

Fig. 19. Drilling holes in a 400 μm 3C–SiC wafer using a femtosecond laser: (a) Top surface of through-hole before cleaning; (b) Top surface of through-hole after cleaning; (c) Bottom of drilled hole [105].

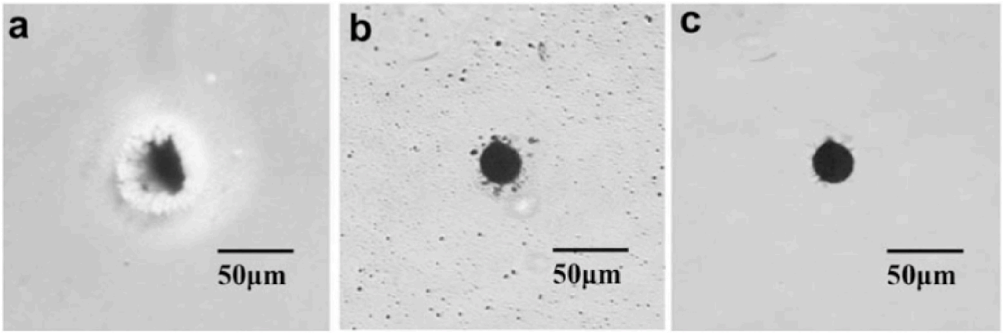

Fig. 20. Drilling holes in 250 μm thick 6H–SiC wafers using a femtosecond laser: (a) Top surface of a microvia hole drilled in air; (b) Top surface of a hole drilled with alcohol assistance; (c) Top surface of through-hole after alcohol cleaning [106].

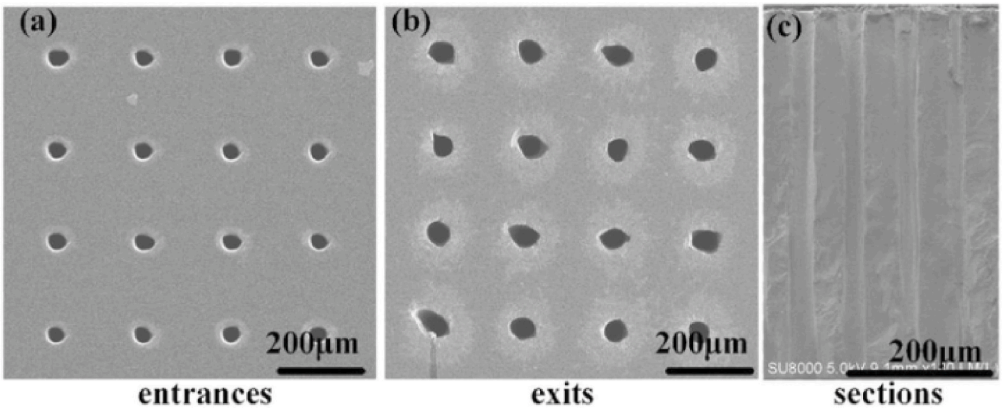

Fig. 21. SEM images of through-hole arrays drilled at a water layer thickness of 500 μm, a pulse book of 40,000, and a pulse energy of 60 μJ: (a) entrances; (b) exitst; and (c) sections [109].

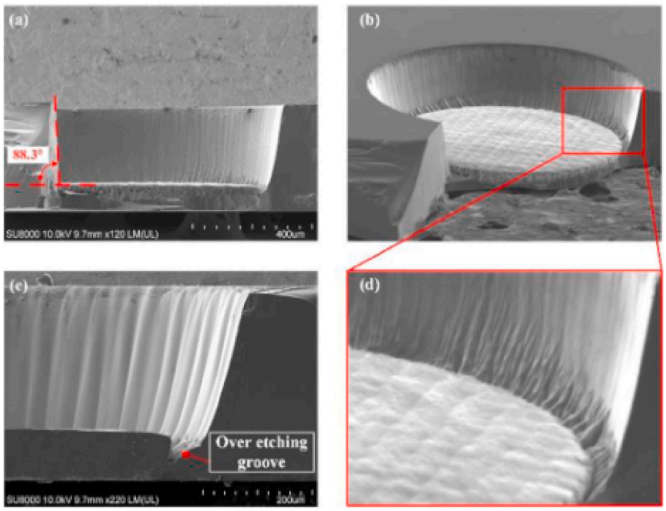

Fig. 22. Blind hole sidewall morphology: (a) cross-section; (b) isometric view; (c) micrograph of over-etched area; (d) micrograph of sidewall bottom [13].

material surfaces induces surface modification and that different structures are formed by varying the laser parameters and conditions. Laser processing is a versatile method for surface patterning [115]. He et al. [116] split an 800 nm, 50 fs femtosecond laser into three laser pulses linearly polarised in different directions to control the periodic ripple structure on the surface of a semiconductor 4H–SiC crystal. This is not possible with conventional single- or double-pulse laser beam irradiation. In contrast to a single pulse, during multi-pulse femtosecond laser processing, each pulse produces ablation on the surface of the material, forming a certain amount of ejecta. Multi-pulse femtosecond laser ablation requires additional factors to be taken into account, such as the shielding effect of the ejecta, the possible buildup of heat from the superposition of the preceding and following pulses, and the effect of pulse spacing. Zhang et al. [117] used an 35 fs, 800 nm laser to ablate the surface of silicon carbide to form micro-nanostructures. It was found that the micro-nanostructure arrays gradually evolved towards V-shaped grooves with the increase of laser fluence, scanning speed or number of scans. The effect of surface roughness on the type of ripple was presented by Chen et al. [118] Under multi-pulse laser irradiation at 515 nm, 290 fs, directional ripple structures are produced in the annealing zone, and deep subwavelength ripples can be produced only on substrates with surface roughness higher than 5.5 nm. In order to deeply investigate the formation process of surface nanostructures, Rehman et al. [119]. irradiated n-type 4H–SiC with 40 fs, 800 nm femtosecond laser pulses under strict focusing conditions to investigate the morphological changes and formation mechanisms induced at and below the surface. It was shown that laser irradiation of SiC induces bond breaking and the transformation of silicon carbide crystals into amorphous silicon (a-Si) and amorphous carbon (a-C). The results show that the complicated interaction between fast laser heating, fusion and fast resolidification, and the dynamic relaxation of laser stress may have played a role in this phenomenon. Long et al. [120]. achieved centimetre-scale, low-damage micromachining of surfaces on single-crystal 4H–SiC substrates using a 240 fs, 515 nm, 75 kHz femtosecond laser using a custom-made diffractive optical element to redistribute the laser pulse energy from Gaussian to square flat-top. It was found that the laser-machined surface was covered with nanoripples and redeposited with nanoparticles. The nanoparticles consisted mainly of amorphous and crystalline silica, and the crystalline silica contained several

different phases. This group [121] also investigated the formation of dense nanostructures on the surface of silicon carbide using a 240 fs, 515 nm femtosecond laser. Fig. 23 shows the morphology and composition of the collected surface nanostructures, which consisted of a large number of silica (SiO_2) nanoparticles with diameters ranging from 5 nm to 30 nm. The width of the surface nanostructured region depends mainly on the number of nanoparticles produced during laser ablation, which increases with increasing laser pulse energy or decreasing laser scanning speed. It was concluded that the nanoparticles produced by laser ablation were decomposed, assembled and oxidised at high temperatures to form cotton-like surface nanostructures. The efficient build-up of nano-particles in the region where the laser irradiation is applied is crucial to forming a cotton-like nanostructure. When treated with low repetition rate laser pulses, effective accumulation does not occur and therefore only flocculated nanostructures can be formed on the laser-treated surface. Shi et al. [122] investigated the structural changes induced by irradiating 4H–SiC targets with a single-pulse femtosecond laser. The results showed that at low energies no structural changes occurred, while at high energies the bonds between crystalline silicon carbide (c-SiC) were broken. These findings deepen the understanding of the formation of surface nanostructures on SiC surfaces by femtosecond laser processing, which facilitates high-quality micromachining of SiC surfaces. In conclusion, for the fabrication of periodic induced structures on WBG materials, picosecond laser processing is faster, but with relatively low precision for applications where large areas need to be processed quickly. Femtosecond lasers can produce nanoscale periodic structures that have higher precision and more complex morphology, allowing for finer material surface modification.

3.2.3. *Laser machining difficult components*

Conventional wire saw technology makes it difficult to cut thin slices from bulk silicon carbide crystals without cutting space, and laser slicing offers a new technical route. Laser slicing of SiC is approximately four times faster than conventional diamond wire saws, making the commercial application of laser stripping of large 4H–SiC wafers possible [123]. Laser slicing also has the advantage of much less kerf loss compared to state-of-the-art wire saws [124]. Wang et al. [125] investigated the effect of surface pretreatment on ultrafast laser cutting of 4H–SiC wafers. A femtosecond laser was used to carry out surface pretreatment on four kinds of 4H–SiC samples with surface roughness of 0.5, 20, 250 and 500 nm, respectively. It was found that the surface pretreatment could reduce the damage to the surface caused by laser processing, promote the stable formation of the modified layer, reduce the solvation area ratio, and lower the tension required for slicing. The modified layer peeling interface is shown in Fig. 24. Xu et al. [126] determined the optimal parameters for cutting SiC wafers using a femtosecond pulsed laser with a pulse width of 130 fs-150 fs, a wavelength of 800 nm, and a repetition frequency of 1 kHz. The bottom of the fs laser cutting has a smooth surface, so that it can decrease the wastage of SiC in cutting.

To avoid creating debris, the researchers sliced the silicon carbide wafer through an invisible cutting technique. Tatsuya Okada et al. [127] observed the formation of the subwavelength periodic strained layers associated with nanoholes in the cross-section of a femtosecond laser illumination within 4H–SiC. Kim et al. [82,128] achieved the exfoliation of 4H–SiC single crystals using femtosecond laser-induced slicing. The study utilised a 780 nm, 220 fs, 1 kHz femtosecond laser to successfully achieve exfoliated surfaces with the root-mean-square roughness of 3 μm and a cutting loss thickness of less than 30 μm. The study also looked at the structure of the exfoliated surface of the SiC crystals. The surface of a stripped sample usually has two areas of different roughness. Typically, 4H–SiC has a solvation plane in the (0001) plane. On the one hand, since the laser cutting was performed in a plane parallel to the dissolved surface, the researchers assumed that the smooth surface region originated from the dissolved plane. On the other hand, in the rough surface region, the researchers assumed that the stripped surface originated from the photoinduced structure. Wang et al. [85,129] investigated the multiple focusing phenomenon of ultra-short pulse lasers in 4H–SiC, and found that under fs conditions, even though there is some self-focusing action in 4H–SiC specimens, it is difficult for the laser to re-focus when dispersed due to the intense plasma defocusing. In contrast, under ps conditions, less plasma is generated at the focal point, and most of the unabsorbed laser light will pass directly through the focal point without being scattered by the plasma. A schematic diagram of the multifocus formation is shown in Fig. 25. Moreover, the lower intensity of the multi-photon absorption loss in the p-state allows for the formation of more and more dense layers at the same energy density.

All of the above studies are about cutting N-type SiC, but silicon carbide can be divided into N-type silicon carbide and semi-insulating silicon carbide. N-type silicon carbide and semi-insulating silicon car-

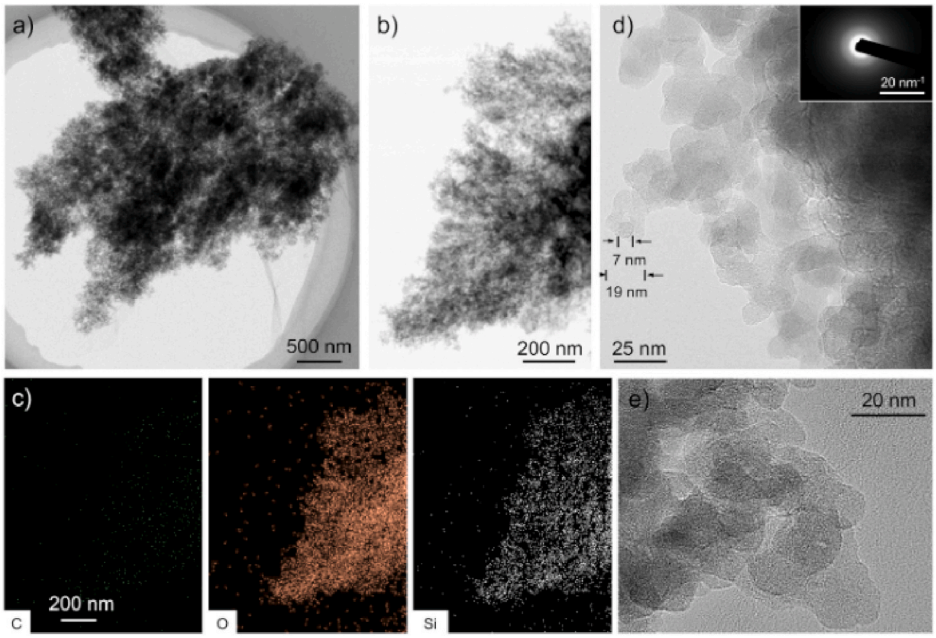

Fig. 23. Surface nanostructures generated at a laser scanning speed of 20 mm/s [121].

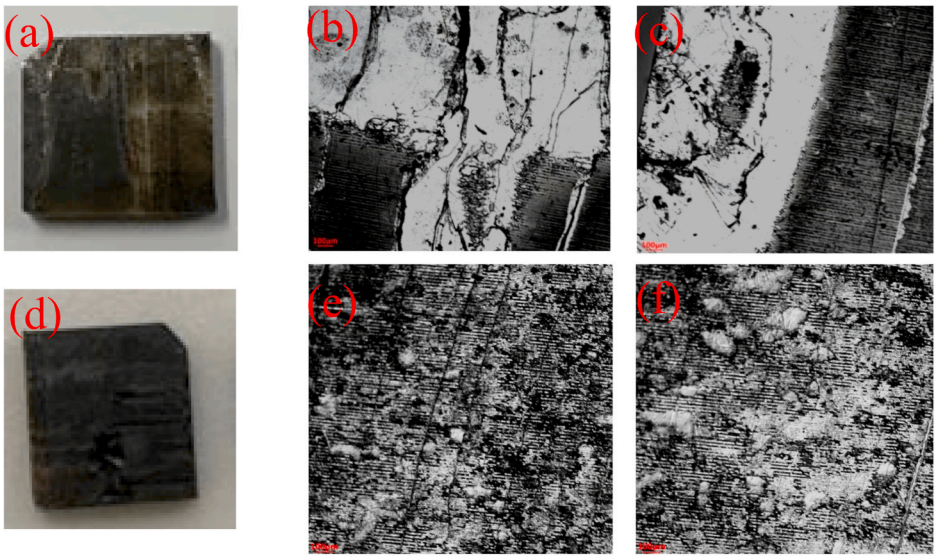

Fig. 24. Microscopic observation of the sample peeling interface [125].

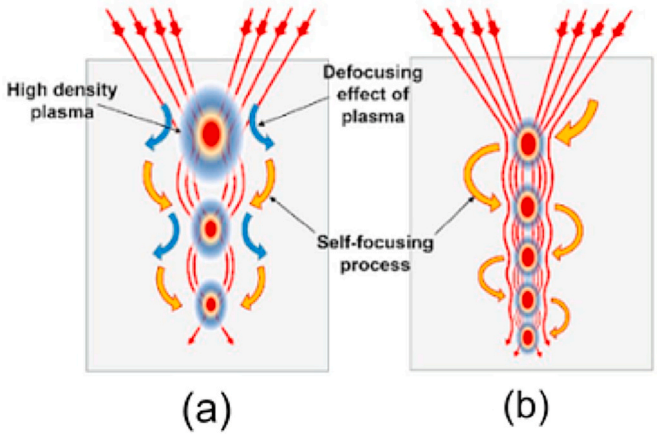

Fig. 25. Schematic of multifocus formation under (a) femtosecond and (b) picosecond pulse width conditions [129].

bide have significantly different resistivity, absorbance and transmittance, and crystallographic orientations, which will have an impact on the process of laser-material interaction during laser slicing. Zhang et al. [130] used a 1030 nm ultrafast laser to fabricate an internal modification layer in semi-insulating silicon carbide that can be used for laser dicing silicon carbide wafers. It is found that internal modification cannot be achieved by femtosecond laser in semi-insulating SiC, but the modified layer is formed more readily with increasing pulse width. The number of modified layers increases with the laser pulse energy and it is proportional to the height and width. These results contribute to the improvement of the slicing quality of semi-insulated silicon carbide wafers.

3.2.4. Other laser processing

Grating structures are attractive because of their suitability for use in silicon carbide optical temperature sensors. Femtosecond micromachined diffraction grating enable the development of optical temperature sensors within transparent bulk 6H–SiC [131]. However, fabricating grating structures with uniform periods of less than a few microns is difficult. Kim et al. [132] prepared parallel deep nanogrooves on 6H–SiC by using 785 nm femtosecond laser. As shown in Fig. 26, the nano-grooves have a high degree of size and pattern uniformity throughout their depth. It is demonstrated that the key parameter for obtaining these deep and regular nanogrooves is the laser fluence. Gao et al. [67] produced grating structures with a uniform period of 1.07 μm on SiC and GaN by optimising the fabrication parameters using an 800 nm, 50 fs laser. The threshold power required to form grating structures on WBG semiconductors was investigated. It was discovered that SiC and GaN have substantially smaller threshold powers than quartz glass. This discrepancy arises because, in contrast to quartz glass, the absorption of incident laser light by SiC and GaN is a low-order nonlinear absorption process.

Using 300 fs, 520 nm femtosecond laser pulses, Guo et al. [133] demonstrated that laser-induced microjet-assisted ablation greatly mitigates the thermal effects of the normal laser ablation process by fabricating microgrooves on the surfaces of single-crystal 4H–SiC wafers and stainless steel strips. Fig. 27 illustrates high-quality microchannels with a large depth-to-width ratio of 5.2 obtained by the laser-induced microjet-assisted ablation single-pass laser scanning process, as well as an array of microchannels fabricated on a 4H–SiC wafer. Wang et al. [134] used a 300 fs, 1035 nm infrared femtosecond laser in the ablation of precisely controllable square grooves with smooth bottoms. A decrease in laser spot overlap in the x-direction has a greater attenuating effect on the material removal rate than in the y-direction. Zhang et al. [135] found that the groove depth, width, heat affected zone and material removal rate in femtosecond laser machining could be accurately predicted by the established regression model.

In addition to the above, there are a number of applications for lasers in silicon carbide processing. Yang et al. [136] proposed a femtosecond laser-based polishing method for reactive bone silicon carbide (RB-SiC). The study was carried out using a 515 nm, 282 fs femtosecond laser on a 5 mm thick RB-SiC material. It is anticipated that some of the conventional mechanical polishing techniques will be replaced by the research, which greatly increases surface quality and polishing efficiency. Aono et al. [137] investigated femtosecond laser modification of single crystal silicon carbide surfaces and its application in microtribology. It was shown that the lubricating properties of the modified layer were improved and the coefficient of friction was 0.01, which was lower than that of the original silicon carbide surface.

Picosecond lasers have better cleanliness, thermal effects and processing accuracy than nanosecond lasers and higher processing efficiency than femtosecond lasers [77]. Laser processing of SiC tends to use laser radiation to modify the surface structure of the material, creating a laser-affected zone that exhibits properties different from those of the original SiC, which is subsequently processed either with assisted processing or with direct laser processing, both of which make the

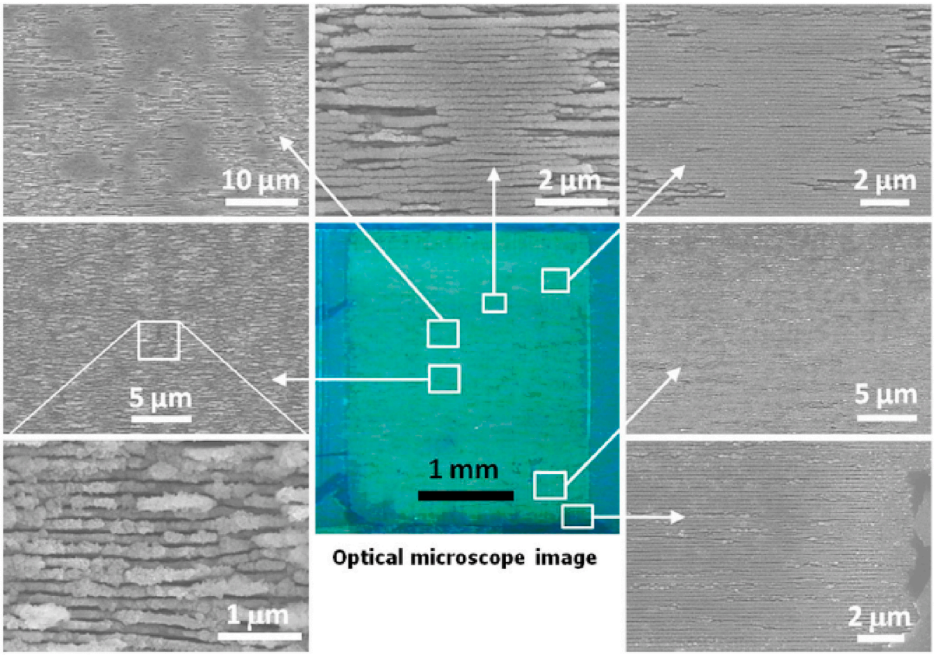

Fig. 26. Fabrication of nanogrooves on 6H–SiC using lasers [132].

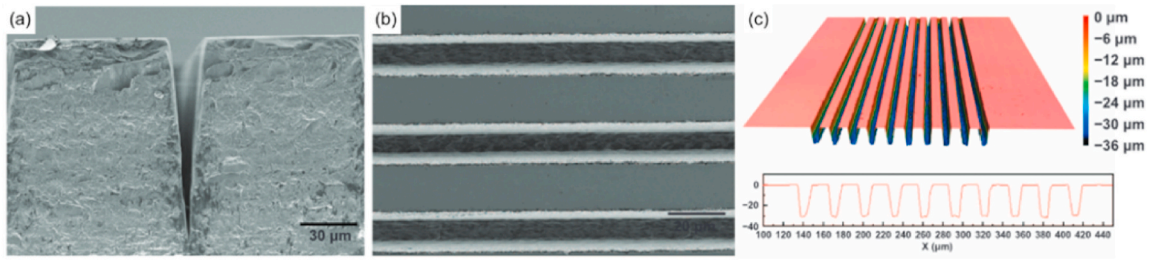

Fig. 27. (a) laser-induced microjet-assisted ablation Side view of microchannels fabricated using a one-pass laser scanning process; (b) Fabrication of microchannel array structure on 4H–SiC wafer; (c) 3D surface profile of the array [133].

processing easier. In summary, ultra-fast laser processing improves the processing rate compared to conventional processes, and can therefore be widely used to fabricate SiC-based MEMS devices, thereby increasing productivity.

4. Ultra-short laser processing of gallium nitride

This chapter describes the application of picosecond and femtosecond lasers for processing gallium nitride materials, where picosecond lasers are mainly used for invisible scribing and laser stripping, and femtosecond lasers are more broadly applicable, including assisted ablation of micro- and nano-structures, laser-induced cyclic surface structures, and laser stripping.

4.1. Picosecond laser processing

Conventional GaN-based devices are mainly grown by heterogeneous epitaxy on rigid substrates and usually sapphire substrates [138]. Laser stripping is favoured by industry due to its non-polluting, stable and convenient characteristics. The conventional laser stripping process usually uses an excimer laser and a nanosecond ultraviolet (UV) laser, since the photon energy of the two sources is greater than the band gap of GaN but less than that of sapphire. Consequently, it is possible to selectively absorb the laser energy in the GaN layer, and to drastically heat the interface area to the thermal delamination temperature. Although this method is feasible, the separated GaN layer still suffers from a large number of defects during actual processing. Sun et al. [139] studied the use of 355 nm , 10 ps picosecond laser irradiation of GaN thin films and gallium nitride-based light-emitting diode (LED) devices to achieve one-step laser stripping, the laser fluence required for stripping is much lower than that of the laser stripping method reported so far, and the surface roughness of the delaminated GaN film can be reduced to 5.2 nm. As can be seen in Fig. 28, the films exhibit a metallic sheen because the gallium and oxides on the surface of the separated gallium nitride films have not been cleaned.

Since the beginning of the 1990s, GaN based materials grown on sapphire substrates have been used to produce high performance blue, green, and UV light emitting diodes. Moser et al. [140] used a 355 nm, 10 ps picosecond laser for pattern definition and material removal in planar GaN-based LEDs. This approach is flexible and accelerates the development and prototyping of new devices. In order to increase market share, the output power of GaN-based LEDs needs to be further increased without increasing production costs. It has been shown that it is possible to increase the output power of LEDs by improving internal quantum efficiency or light extraction efficiency. The most common method to enhance the light extraction efficiency is to roughen or shape the GaN epitaxial layer. Chang et al. [141] proposed a simple shifted laser stealth dicing method to enhance the output power of GaN-based blue LEDs. Two additional picosecond laser shifts were required at different locations on the backside compared to the conventional

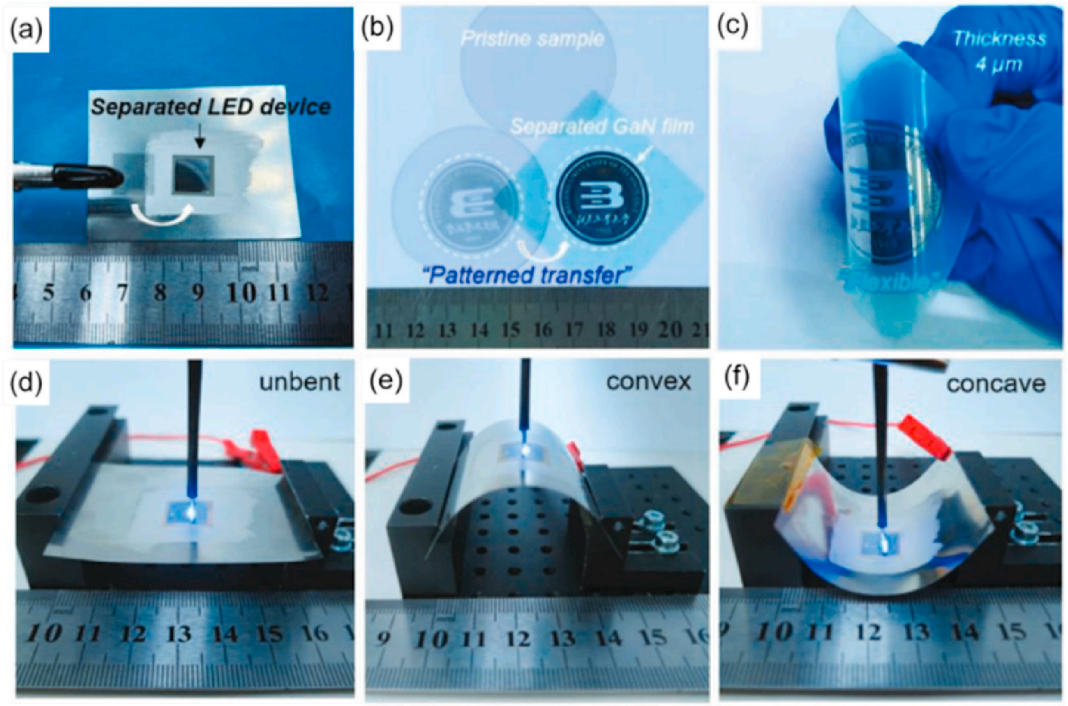

Fig. 28. (a) Photograph of a separated LED device; (b–c) Patterned GaN film attached to a TRT substrate; (d–f) Optical images of violet-blue EL from the separated LED device under different bending states [139].

method of only 1 ns laser shifting from the front side. Passow et al. [142] reported the repair of defects in GaN-based LEDs by UV laser micromachining. Impact and helical drilling in GaN was studied using 248 nm and 355 nm picosecond pulsed laser ablation. The effect of laser ablation on the optoelectronic properties of GaN-based LED chips with different laser parameters was investigated.

4.2. Femtosecond laser processing

When processing GaN using femtosecond laser ablation, the higher energy density of the fs laser is usually utilised to achieve material removal by ablation. In order to improve the smoothness of the surface microstructure of GaN materials after femtosecond laser processing, Nakashima's group [143] adjusted the size of the ablation crater and surface roughness by using HCl solution etching treatment or changing the parameters of femtosecond laser processing after femtosecond laser irradiation. The results show that the roughness of GaN surface microstructure is effectively changed by HCl solution treatment, and the results are shown in Fig. 29. After laser irradiation, Ga-rich phases with metallic luster were generated in the laser irradiated area, and the ratio of Ga to N was increased from 1.56 to 1.82. Subsequently, the Ga-rich phases were removed by chemical etching using HCl solution, and the roughness of the laser-irradiated surface was effectively reduced. However, due to the high bonding energy of GaN and its strong chemical stability, it is difficult to use HCl solution to etch the Ga-rich phase. Therefore, it is difficult to use HCl solution to effectively etch the ablation crater after femtosecond laser irradiation, and it is difficult to obtain a satisfactory etching rate to form high-quality optical microstructures. In order to further investigate the effect of femtosecond laser processing parameters on the surface smoothness of the ablation crater, Nakashima's group [34,144] used two different wavelengths of femtosecond laser, 775 nm and 387 nm, as well as the number of pulses to process the GaN materia. The researchers used a 775 nm laser to focus a single pulse onto the surface of GaN material by scanning to obtain microstructures, and investigated the variation rule of the diameter and depth of microstructures with the pulse energy. The experimental results show that when the pulse energy is less than 200 nJ, the diameter and depth of the microstructure grow rapidly with the increase of pulse energy; when the pulse energy is more than 200 nJ, the diameter and depth of the microstructure tend to stabilise with the increase of pulse energy. It was found that the ablation crater formed on the surface of GaN material by femtosecond laser irradiation and then processed with HCl solution did not substantially increase the diameter of the ablation crater, while changing the parameters of femtosecond laser processing

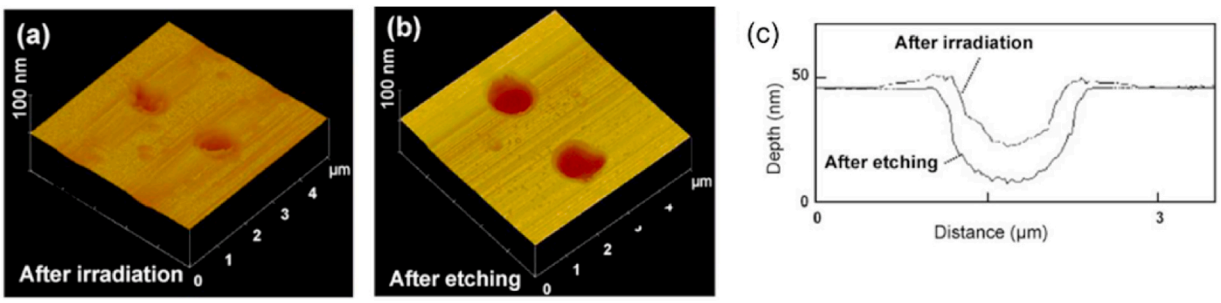

Fig. 29. AFM images of ablation craters on GaN surface: (a) topography after laser irradiation; (b) topography after HCl etching; (c) cross-section contours [143].

can increase the diameter and depth of the ablation crater. Although the results did not achieve the preparation of microstructures with a certain shape and appearance on the GaN surface, they showed a way to influence the microstructure by removing the laser irradiated area through selective etching. Ou et al. [37] used a femtosecond laser irradiation of GaN at 800 nm, 30 fs, and 1 kHz, and then wet etching to prepare hexagonal microstructures on the Ga pole surface of the GaN material. The experimental results show that the depth and pore size of the microstructures increase with the increase of laser energy applied to the GaN surface. When the laser energy is 2 mW, the hexagonal microstructure of the laser is more regular. In addition, the law of change of the etched aperture with the etching time under different laser energies shows that the 4h before the etching is the main factor for deciding the size of the diameter of the microstructures, and the change of the laser energy does not have much influence on the etching rate.

In addition to the use of other technologies to assist femtosecond laser micromachining of GaN, in recent years, femtosecond laser direct writing GaN micromachining has also been a lot of research. Wang et al. [145] used a femtosecond laser with 150 fs, 775 nm, 250 Hz, and an approximate Gaussian shape of the beam profile to process a laser-induced periodic surface structure on a GaN/sapphire surface. It is found that the incident laser energy laser induces an effect on the period of the ripples. Miyaji et al. [146] formed uniform nanogratings with a period of 50 nm on GaN in air by two-step ablation using a 266 nm, 100 fs, 10 Hz UV femtosecond laser pulse. Yulianto et al. [147] processed InGaN/GaN-based light-emitting diodes on sapphire substrates and transferred them to a foreign substrate (copper foil) by a two-step transfer method using a 520 nm femtosecond laser. Voronenkov et al. [148] used a 350 fs, 1030 nm, 400 μJ near-infrared femtosecond laser pulse focusing technique to cut GaN films with an epitaxial device structure from an exotic GaN substrate. The luminescence image of the LED chip on the copper substrate is shown in Fig. 30, which proves that the structure was not damaged during the laser stripping process. Yulianto et al. [16] used nonlinear absorption of 520 nm, 350 fs, 200 kHz femtosecond laser for laser lift-off (LLO). But the non-linear effect of multi-photon absorption induced GaN layer separation method has led to higher manufacturing costs for GaN-based devices. Moreover, the MLR of the GaN layers isolated with this approach is even poorer than those obtained from the conventional separation. Nolasco et al. [149] investigated the incubation effect during femtosecond laser microfabrication of GaN thin films at three different wavelengths, and the incubation curves are shown in Fig. 31. The results show that micromachining is mainly determined by multiphoton ionization at 343 nm and 515 nm, and other effects such as tunneling ionization at 1030 nm. As the irradiation wavelength increases, two-photon or multiphoton absorption dominates. The two/multiphoton absorption induces significant fluctuations in the GaN ablation threshold, which undoubtedly puts higher demands on the regulation of the laser pulse energy. Wei et al. [17] systematically investigated the effects and interactions of parameters on GaN processing, and achieved efficient and nearly damage-free micromachining of GaN using femtosecond laser direct writing technology by means of a quadratic polynomial prediction model established.

When processing GaN by laser ablation, the higher energy density of the laser is usually utilised to achieve ablative removal of the material. The size of the laser energy affects the size of the laser ablation craters and the laser-modified area due to the difference in laser energy acting on the GaN surface after laser processing. On the other hand, the multiphoton absorption of the laser nonlinear effect increases the cost of the actual production of GaN-based devices, which puts higher demands on the regulation of the laser pulse energy. Compared with the conventional method, ultrafast laser treatment can significantly reduce the light-matter interaction time, reduce the light-matter interaction, and reduce the heat accumulation in the LLO process [150]. At the same time, high costs are inevitable. In contrast, it may be more cost-effective to use other techniques to assist laser micromachining of GaN.

5. Conclusions and outlooks

This review summarises the application of ultra-short pulsed laser for processing silicon carbide and gallium nitride materials and the physical mechanisms of interaction with semiconductor materials. Ultra-short pulse laser can effectively reduce the heat-affected zone due to their ultrashort interaction time. The pulse delivers its energy through photon-electron coupling before phonons drive thermal diffusion. Ultrafast laser processing has a wide range of applications due to its unique non-linear absorption and non-thermal properties. As the semiconductor industry's demand for efficient and precise manufacturing continues to grow, ultrafast laser processing technology is expected to find wider application. Traditional semiconductor material processing methods are

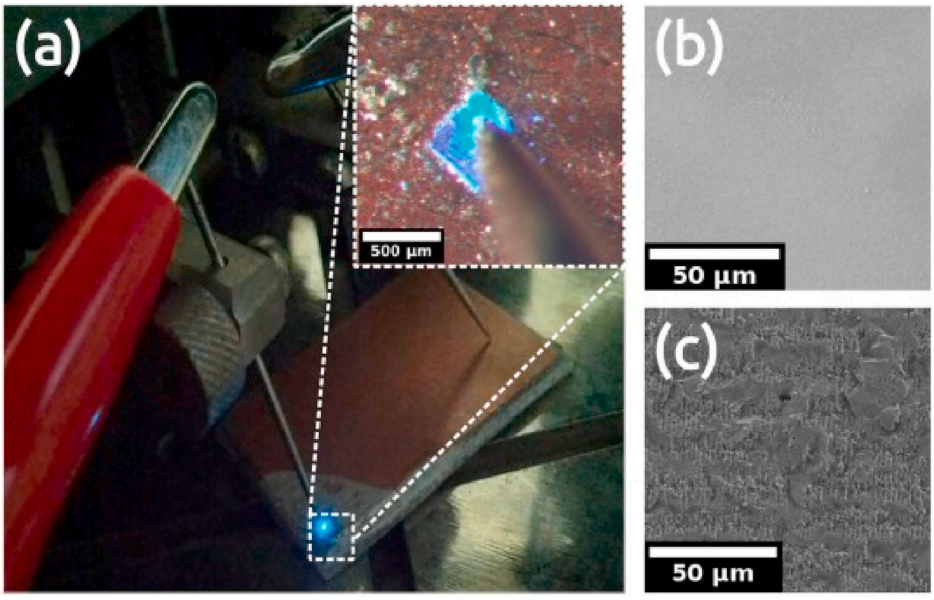

Fig. 30. (a) InGaN LED chip on copper substrate electroluminescence under operating current; SEM image of (b) Ga/(c) N side of the chip after laser stripping process [148].

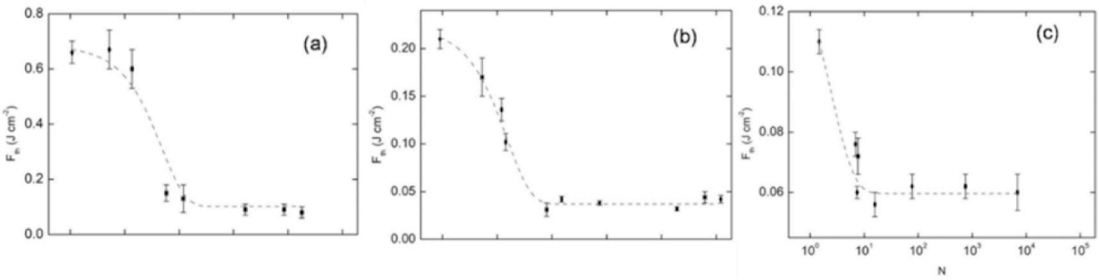

Fig. 31. Incubation curves of GaN at (a)1030 nm, (b) 515 nm and (c)343 nm laser pulses [149].

often limited by the nature of the material, processing equipment and other factors, it is difficult to realize some specific processing needs. Ultra-fast laser processing technology has a higher degree of flexibility and controllability, according to different processing needs to adjust the laser parameters, to achieve diversified processing results. At the same time, compared with traditional processing methods, ultrafast laser processing speed is faster, higher precision, help promote the further development of semiconductor material processing. In conclusion, both picosecond and femtosecond ultra-short pulse lasers can be used as the first choice for processing WBG semiconductor materials such as SiC and GaN. With their low thermal effects, small heat-affected zones, and precise control of the processing geometry, they are an excellent choice for micro- and nano-processing.

In terms of processing SiC, there are many research reports on ultrafast lasers, which can be summarized into three main areas. First, the use of femtosecond laser-assisted processing. Mainly SiC belongs to the ultra-hard and difficult to process materials, traditional mechanical processing is more difficult, through the laser irradiation surface modification can be easy to process. Second, the use of ultrafast laser manufacturing micron or nanometer structure, such as through holes, thin films, surface structure. Third, the use of ultrafast laser processing instead of traditional processes, such as laser cutting, laser polishing, etc., significantly improve the surface quality and efficiency. On the other hand, the unique substrate production method of GaN materials makes ultrafast laser processing uniquely useful for laser stripping. Ultra-fast laser processing significantly reduces the interaction time between light and material, thus reducing the heat build-up during laser stripping and obtaining a high-quality stripped surface.

Future research on ultrafast laser processing of wide-band semiconductor materials still has some difficulties.

1. At the same laser energy density, femtosecond lasers are more accurate and picosecond lasers are more efficient. For femtosecond pulses, mode-locking is almost the only means of realization, and thus relatively lower cost for picosecond lasers. Nonlinear effects such as multiphoton ionization dominate when ultrashort pulsed lasers interact with transparent media. Femtosecond lasers are more likely to reach the nonlinear threshold and are more adaptable to the absorption properties of the material. Therefore, femtosecond pulsed lasers are more advantageous in transparent medium processing and other occasions. In the selection of laser parameters, the influence of thermal effects, cost, application scenarios should be considered comprehensively, and the appropriate pulse width should be selected in the balance between efficiency and precision;
2. The trend in femtosecond laser technology is towards high-precision processing, with the disadvantage of not being able to achieve high-volume processing comparable to traditional microelectronic/microelectromechanical manufacturing technologies, and exploring new strategies such as parallel multi-beam processing and volumetric fabrication technologies to improve processing efficiency is also a direction that meets the criteria for high-volume production;
3. Most of the current research has focused on distributing the laser energy density in the spot according to a Gaussian distribution, and few other types of beam processing have been studied;
4. Whether picosecond or femtosecond, the mechanism of interaction between ultrafast lasers and semiconductor materials is still unclear, which calls for a deeper investigation of the interaction mechanism and the need to propose more accurate physical models.

At present, as the smallest feature size achievable by micromachining technology continues to decrease, further improvement of machining accuracy and quality has been the challenge to be broken through. The excellent performance of ultrafast laser processing technology in the field of micromachining has received more and more attention from the industry and scholars. In recent years, SiC and GaN have gradually gained widespread attention and application in the field of semiconductor materials. The booming semiconductor industry and the pursuit of higher performance materials will surely lead to the same rapid development of processing methods. One of the key areas of future research in ultrafast laser processing is the establishment of a multi-beam parallel processing system, which will enable the industrial productivity of ultrafast laser processing to be greatly enhanced. In addition, the study of laser beam morphology will allow for more precise processing results. Future researchers will be able to use lasers to process wide-band semiconductor materials more efficiently and with higher quality.

CRediT authorship contribution statement

Keran Jiang: Writing – original draft, Methodology, Investigation, Formal analysis, Conceptualization. **Peilei Zhang:** Writing – review & editing, Visualization, Validation, Investigation, Funding acquisition. **Shijie Song:** Writing – review & editing, Supervision, Investigation, Data curation. **Tianzhu Sun:** Investigation. **Yu Chen:** Investigation. **Haichuan Shi:** Writing – review & editing. **Hua Yan:** Writing – review & editing. **Qinghua Lu:** Visualization. **Guanglong Chen:** Funding acquisition.

Declaration of competing interest

The authors declare that they have no known competing financial interests or personal relationships that could have appeared to influence the work reported in this paper.

Data availability

No data was used for the research described in the article.

Acknowledgements

This research was supported by Foundation of Natural Science Foundation of China (52075317, 12174247), Class III Peak Discipline of Shanghai—Materials Science and Engineering (High-Energy Beam

Intelligent Processing and Green Manufacturing).

References

[1] J. Ballestín-Fuertes, J. Muñoz-Cruzado-Alba, J. Sanz-Osorio, E. Laporta-Puyal, Role of wide bandgap materials in power electronics for smart grids applications, Electronics 10 (2021) 677, https://doi.org/10.3390/electronics10060677.

[2] M. Chambonneau, D. Grojo, O. Tokel, F.Ö. Ilday, S. Tzortzakis, S. Nolte, In-volume laser direct writing of silicon—challenges and opportunities, Laser Photon. Rev. 15 (2021) 2100140, https://doi.org/10.1002/lpor.202100140.

[3] X. Wang, X. Yu, H. Shi, X. Tian, M. Chambonneau, D. Grojo, B. DePaola, M. Berg, S. Lei, Characterization and control of laser induced modification inside silicon, J. Laser Appl. 31 (2019) 022601, https://doi.org/10.2351/1.5096086.

[4] O. Tokel, A. Turnalı, G. Makey, P. Elahi, T. Çolakoğlu, E. Ergeçen, Ö. Yavuz, R. Hübner, M. Zolfaghari Borra, I. Pavlov, A. Bek, R. Turan, D.K. Kesim, S. Tozburun, S. Ilday, F.Ö. Ilday, In-chip microstructures and photonic devices fabricated by nonlinear laser lithography deep inside silicon, Nature Photon 11 (2017) 639–645, https://doi.org/10.1038/s41566-017-0004-4.

[5] X. Yu, X. Wang, M. Chanal, C.A. Trallero-Herrero, D. Grojo, S. Lei, Internal modification of intrinsic and doped silicon using infrared nanosecond laser, Appl. Phys. A 122 (2016) 1001, https://doi.org/10.1007/s00339-016-0540-7.

[6] X. Wang, L. Trinh, X. Yu, M. Berg, S. Hosseini-Zavareh, B. Lacroix, P. Chen, R. Chen, B. Cui, S. Lei, Direct observation and quantification of nanosecond laser induced amorphization inside silicon, J. Laser Appl. 36 (2024), https://doi.org/10.2351/7.0001305.

[7] D. Grojo, A. Mouskeftaras, P. Delaporte, S. Lei, Limitations to laser machining of silicon using femtosecond micro-Bessel beams in the infrared, J. Appl. Phys. 117 (2015) 153105, https://doi.org/10.1063/1.4918669.

[8] X. Wang, X. Yu, M. Berg, P. Chen, B. Lacroix, S. Fathpour, S. Lei, Curved waveguides in silicon written by a shaped laser beam, Opt Express 29 (2021) 14201, https://doi.org/10.1364/OE.419074.

[9] M. Chambonneau, X. Wang, X. Yu, Q. Li, D. Chaudanson, S. Lei, D. Grojo, Positive- and negative-tone structuring of crystalline silicon by laser-assisted chemical etching, Opt Lett 44 (2019) 1619–1622, https://doi.org/10.1364/OL.44.001619.

[10] P. Wang, P. Ge, M. Ge, W. Bi, J. Meng, Material removal mechanism and crack propagation in single scratch and double scratch tests of single-crystal silicon carbide by abrasives on wire saw, Ceram. Int. 45 (2019) 384–393, https://doi.org/10.1016/j.ceramint.2018.09.178.

[11] Y. Chen, C. Zhang, L. Li, S. Zhou, X. Chen, J. Gao, N. Zhao, C.-P. Wong, Hybrid anodic and metal-assisted chemical etching method enabling fabrication of silicon carbide nanowires, Small 15 (2019) 1803898, https://doi.org/10.1002/smll.201803898.

[12] J. Li, D. Geng, D. Zhang, W. Qin, Y. Jiang, Ultrasonic vibration mill-grinding of single-crystal silicon carbide for pressure sensor diaphragms, Ceram. Int. 44 (2018) 3107–3112, https://doi.org/10.1016/j.ceramint.2017.11.077.

[13] Y. Zhao, Y.-L. Zhao, L.-K. Wang, Application of femtosecond laser micromachining in silicon carbide deep etching for fabricating sensitive diaphragm of high temperature pressure sensor, Sensor Actuator Phys. 309 (2020) 112017, https://doi.org/10.1016/j.sna.2020.112017.

[14] A. Najar, M. Shafa, D. Anjum, Synthesis, optical properties and residual strain effect of GaN nanowires generated via metal-assisted photochemical electroless etching, RSC Adv. 7 (2017) 21697–21702, https://doi.org/10.1039/C7RA02348K.

[15] H.W. Choi, E. Gu, C. Liu, J.M. Girkin, M.D. Dawson, Fabrication and evaluation of GaN negative and bifocal microlenses, J. Appl. Phys. 97 (2005) 063101, https://doi.org/10.1063/1.1857062.

[16] N. Yulianto, G.T.M. Kadja, S. Bornemann, S. Gahlawat, N. Majid, K. Triyana, F. F. Abdi, H.S. Wasisto, A. Waag, Ultrashort pulse laser lift-off processing of inGaN/GaN light-emitting diode chips, ACS Appl. Electron. Mater. 3 (2021) 778–788, https://doi.org/10.1021/acsaelm.0c00913.

[17] H. Wei, C. Huang, H. Liu, D. Liu, P. Yao, D. Chu, Modeling and optimizing femtosecond laser process parameters for high-efficient and near damage-free micromachining of single-crystal GaN substrate, Mater. Sci. Semicond. Process. 153 (2023) 107123, https://doi.org/10.1016/j.mssp.2022.107123.

[18] R. Kirschman, Status of silicon carbide (SiC) as a WideBandgap semiconductor for HighTemperature applications: a review, in: High-Temperature Electronics, IEEE, 1999, pp. 511–524, https://doi.org/10.1109/9780470544884.ch69.

[19] T. Kimoto, 2 - SiC material properties, in: B.J. Baliga (Ed.), Wide Bandgap Semiconductor Power Devices, Woodhead Publishing, 2019, pp. 21–42, https://doi.org/10.1016/B978-0-08-102306-8.00002-2.

[20] M. Ahn, R. Cahyadi, J. Wendorf, W. Bowen, B. Torralva, S. Yalisove, J. Phillips, Low damage electrical modification of 4H-SiC via ultrafast laser irradiation, J. Appl. Phys. 123 (2018) 145106, https://doi.org/10.1063/1.5020445.

[21] D. Shi, Y. Chen, Z. Li, S. Dong, L. Li, M. Hou, H. Liu, S. Zhao, X. Chen, C.-P. Wong, N. Zhao, Anisotropic charge transport enabling high-throughput and high-aspect-ratio wet etching of silicon carbide, Small Methods 6 (2022) 2200329, https://doi.org/10.1002/smtd.202200329.

[22] Y. Okamoto, T. Okubo, A. Kajitani, A. Okada, High-quality micro-shape fabrication of monocrystalline diamond by nanosecond pulsed laser and acid cleaning, Int. J. Extrem. Manuf. 4 (2022) 025301, https://doi.org/10.1088/2631-7990/ac5a6a.

[23] S. Gupta, Pulsed laser ablation and micromachining of 4H and 6H SiC wafers for high-temperature MEMS sensors, in: Ames, 2008 2807136, https://doi.org/10.31274/etd-180810-2407.

[24] A.A. Lyalin, E.D. Obraztsova, A.V. Simakin, I.I. Vlasov, G.A. Shafeev, Pulsed laser activation and electroless metallization of SiC single crystal, in: 1998 Fourth International High Temperature Electronics Conference. HITEC (Cat. No.98EX145), 1998, pp. 308–312, https://doi.org/10.1109/HITEC.1998.676810.

[25] R.F. Wood, D.H. Lowndes, Laser processing of wide bandgap semiconductors and insulatorsCryst. Lattice defects amorphous mater, lattice defects amorphous, Mater 12 (1985) 475–497.

[26] T. Blank, Y.A. Goldberg, O.V. Konstantinov, Temperature dependence of the performance of ultraviolet detectors, Nucl. Instrum. Methods Phys. Res. Sect. A Accel. Spectrom. Detect. Assoc. Equip. 509 (2003) 109–117, https://doi.org/10.1016/S0168-9002(03)01558-4.

[27] B. Pecholt, M. Vendan, Y. Dong, P. Molian, Ultrafast laser micromachining of 3C-SiC thin films for MEMS device fabrication, Int. J. Adv. Manuf. Technol. 39 (2008) 239–250, https://doi.org/10.1007/s00170-007-1223-5.

[28] S. Zoppel, M. Farsari, R. Merz, J. Zehetner, G. Stangl, G.A. Reider, C. Fotakis, Laser micro machining of 3C–SiC single crystals, Microelectron. Eng. 83 (2006) 1400–1402, https://doi.org/10.1016/j.mee.2006.01.064.

[29] J.-P. Desbiens, P. Masson, ArF excimer laser micromachining of Pyrex, SiC and PZT for rapid prototyping of MEMS components, Sensor Actuator Phys. 136 (2007) 554–563, https://doi.org/10.1016/j.sna.2007.01.002.

[30] C. Merz, M. Kunzer, U. Kaufmann, I. Akasaki, H. Amano, Free and bound excitons in thin wurtzite GaN layers on sapphire, Semicond. Sci. Technol. 11 (1996) 712–716, https://doi.org/10.1088/0268-1242/11/5/010.

[31] T. Sochacki, M. Amilusik, B. Lucznik, M. Bockowski, J. Weyher, G. Nowak, B. Sadovyi, G. Kamler, I. Grzegory, R. Kucharski, M. Zajac, R. Doradzinski, R. Dwiliński, HVPE-GaN growth on ammonothermal GaN crystals, Proc. SPIE-Int. Soc. Opt. Eng. 8625 (2013), https://doi.org/10.1117/12.2003699.

[32] F. Schubert, U. Merkel, T. Mikolajick, S. Schmult, Influence of substrate quality on structural properties of AlGaN/GaN superlattices grown by molecular beam epitaxy, J. Appl. Phys. 115 (2014) 083511, https://doi.org/10.1063/1.4866718.

[33] S. Strite, H. Morkoç, GaN, AlN, and InN: a review, J. Vac. Sci. Technol. B: Microelectronics and Nanometer Structures 10 (1992) 1237–1266, https://doi.org/10.1116/1.585897.

[34] S. Nakashima, Improvement of resolution in nano-fabrication of GaN by wet-chemical-assisted femtosencond laser ablation, Journal of Laser Micro Nanoengineering - J LASER MICRO NANOENG 5 (2010) 21–24, https://doi.org/10.2961/jlmn.2010.01.0005.

[35] S.J. Pearton, R.J. Shul, F. Ren, A review of dry etching of GaN and related materials, MRS Internet J. Nitride Semicond. Res. 5 (2020) 11, https://doi.org/10.1557/S1092578300000119.

[36] D. Zhuang, J.H. Edgar, Wet etching of GaN, AlN, and SiC: a review, materials science and engineering: r, Reports 48 (2005) 1–46, https://doi.org/10.1016/j.mser.2004.11.002.

[37] Y. Ou, C. Li, J. Qian, Y. Xiao, S. Li, Z. Feng, Fabrication of hexagonal microstructure on gallium nitride films by wet etching assisted femtosecond laser ablation, Opt Commun. 528 (2023) 128952, https://doi.org/10.1016/j.optcom.2022.128952.

[38] R. Srinivasan, E. Sutcliffe, B. Braren, Ablation and etching of polymethylmethacrylate by very short (160 fs) ultraviolet (308 nm) laser pulses, Appl. Phys. Lett. 51 (1987) 1285–1287, https://doi.org/10.1063/1.99001.

[39] S. Küper, M. Stuke, Femtosecond uv excimer laser ablation, Appl. Phys. B 44 (1987) 199–204, https://doi.org/10.1007/BF00692122.

[40] R.R. Gattass, E. Mazur, Femtosecond laser micromachining in transparent materials, Nature Photon 2 (2008) 219–225, https://doi.org/10.1038/nphoton.2008.47.

[41] K. Sugioka, Y. Cheng, Ultrafast lasers—reliable tools for advanced materials processing, Light Sci. Appl. 3 (2014), https://doi.org/10.1038/lsa.2014.30 e149–e149.

[42] W. Zhang, P. Zhang, H. Yan, R. Li, H. Shi, D. Wu, T. Sun, Z. Luo, Y. Tian, Research status of femtosecond lasers and nanosecond lasers processing on bulk metallic glasses (BMGs), Opt Laser. Technol. 167 (2023) 109812, https://doi.org/10.1016/j.optlastec.2023.109812.

[43] M.F. Yanik, H. Cinar, H.N. Cinar, A.D. Chisholm, Y. Jin, A. Ben-Yakar, Functional regeneration after laser axotomy, Nature 432 (2004), https://doi.org/10.1038/432822a, 822–822.

[44] N. Bärsch, K. Koerber, A. Ostendorf, K.H. Tönshoff, Ablation and cutting of planar silicon devices using femtosecond laser pulses, Appl. Phys. A 77 (2003) 237–242, https://doi.org/10.1007/s00339-003-2118-4.

[45] C. Momma, B.N. Chichkov, S. Nolte, F. Von Alvensleben, A. Tünnermann, H. Welling, B. Wellegehausen, Short-pulse laser ablation of solid targets, Opt Commun. 129 (1996) 134–142, https://doi.org/10.1016/0030-4018(96)00250-7.

[46] A. Rousse, C. Rischel, S. Fourmaux, I. Uschmann, S. Sebban, G. Grillon, P. Balcou, E. Förster, J.P. Geindre, P. Audebert, J.C. Gauthier, D. Hulin, Non-thermal melting in semiconductors measured at femtosecond resolution, Nature 410 (2001) 65–68, https://doi.org/10.1038/35065045.

[47] M. Hase, P. Fons, K. Mitrofanov, A.V. Kolobov, J. Tominaga, Femtosecond structural transformation of phase-change materials far from equilibrium monitored by coherent phonons, Nat. Commun. 6 (2015) 8367, https://doi.org/10.1038/ncomms9367.

[48] H.M. null van Driel, Kinetics of high-density plasmas generated in Si by 1.06- and 0.53- microm picosecond laser pulses, Phys. Rev. B Condens. Matter 35 (1987) 8166–8176, https://doi.org/10.1103/physrevb.35.8166.

[49] N.M. Bulgakova, R. Stoian, A. Rosenfeld, I.V. Hertel, E.E.B. Campbell, Electronic transport and consequences for material removal in ultrafast pulsed laser ablation

of materials, Phys. Rev. B 69 (2004) 054102, https://doi.org/10.1103/PhysRevB.69.054102.
[50] B.C. Stuart, M.D. Feit, S. Herman, A.M. Rubenchik, B.W. Shore, M.D. Perry, Nanosecond-to-femtosecond laser-induced breakdown in dielectrics, Phys. Rev. B 53 (1996) 1749–1761, https://doi.org/10.1103/PhysRevB.53.1749.
[51] K. Sokolowski-Tinten, J. Bialkowski, A. Cavalleri, D. von der Linde, A. Oparin, J. Meyer-ter-Vehn, S.I. Anisimov, Transient states of matter during short pulse laser ablation, Phys. Rev. Lett. 81 (1998) 224–227, https://doi.org/10.1103/PhysRevLett.81.224.
[52] L. Rapp, B. Haberl, C.J. Pickard, J.E. Bradby, E.G. Gamaly, J.S. Williams, A. V. Rode, Experimental evidence of new tetragonal polymorphs of silicon formed through ultrafast laser-induced confined microexplosion, Nat. Commun. 6 (2015) 7555, https://doi.org/10.1038/ncomms8555.
[53] A.Y. Vorobyev, C. Guo, Direct femtosecond laser surface nano/microstructuring and its applications, Laser Photon. Rev. 7 (2013) 385–407, https://doi.org/10.1002/lpor.201200017.
[54] G. Paltauf, P.E. Dyer, Photomechanical processes and effects in ablation, Chem. Rev. 103 (2003) 487–518, https://doi.org/10.1021/cr010436c.
[55] N.M. Bulgakova, A.V. Bulgakov, Pulsed laser ablation of solids: transition from normal vaporization to phase explosion, Appl Phys A 73 (2001) 199–208, https://doi.org/10.1007/s003390000686.
[56] M.V. Shugaev, C. Wu, O. Armbruster, A. Naghilou, N. Brouwer, D.S. Ivanov, T.J.-Y. Derrien, N.M. Bulgakova, W. Kautek, B. Rethfeld, L.V. Zhigilei, Fundamentals of ultrafast laser–material interaction, MRS Bull. 41 (2016) 960–968, https://doi.org/10.1557/mrs.2016.274.
[57] H.M. van Driel, Kinetics of high-density plasmas generated in Si by 1.06- and 0.53-\ensuremath{\mu}m picosecond laser pulses, Phys. Rev. B 35 (1987) 8166–8176, https://doi.org/10.1103/PhysRevB.35.8166.
[58] E. Leveugle, D.S. Ivanov, L.V. Zhigilei, Photomechanical spallation of molecular and metal targets: molecular dynamics study, Appl Phys A 79 (2004) 1643–1655, https://doi.org/10.1007/s00339-004-2682-2.
[59] C. Wu, M.S. Christensen, J.-M. Savolainen, P. Balling, L.V. Zhigilei, Generation of subsurface voids and a nanocrystalline surface layer in femtosecond laser irradiation of a single-crystal Ag target, Phys. Rev. B 91 (2015) 035413, https://doi.org/10.1103/PhysRevB.91.035413.
[60] C. Wu, L.V. Zhigilei, Microscopic mechanisms of laser spallation and ablation of metal targets from large-scale molecular dynamics simulations, Appl. Phys. A 114 (2014) 11–32, https://doi.org/10.1007/s00339-013-8086-4.
[61] S.S. Harilal, J.R. Freeman, P.K. Diwakar, A. Hassanein, Femtosecond laser ablation: fundamentals and applications, in: S. Musazzi, U. Perini (Eds.), Laser-Induced Breakdown Spectroscopy: Theory and Applications, Springer, Berlin, Heidelberg, 2014, pp. 143–166, https://doi.org/10.1007/978-3-642-45085-3_6.
[62] W.G. Roeterdink, L.B.F. Juurlink, O.P.H. Vaughan, J. Dura Diez, M. Bonn, A. W. Kleyn, Coulomb explosion in femtosecond laser ablation of Si(111), Appl. Phys. Lett. 82 (2003) 4190–4192, https://doi.org/10.1063/1.1580647.
[63] J. Reif, M. Henyk, D. Wolfframm, Explosive femtosecond ablation from ionic crystals, in: Laser Applications in Microelectronic and Optoelectronic Manufacturing V, SPIE, 2000, pp. 26–33, https://doi.org/10.1117/12.387576.
[64] R. Stoian, D. Ashkenasi, A. Rosenfeld, E. Campbell, Coulomb explosion in ultrashort pulsed laser ablation of Al2O3, Physical Review B - PHYS REV B 621 (2000), https://doi.org/10.1103/PhysRevB.62.13167, 78183–13173.
[65] N.M. Bulgakova, A.V. Bulgakov, V.P. Zhukov, W. Marine, A.Y. Vorobyev, C. Guo, Charging and plasma effects under ultrashort pulsed laser ablation, in: High-Power Laser Ablation VII, SPIE, 2008, pp. 105–119, https://doi.org/10.1117/12.782643.
[66] M. Ams, G.D. Marshall, P. Dekker, M. Dubov, V.K. Mezentsev, I. Bennion, M. J. Withford, Investigation of ultrafast laser–photonic material interactions: challenges for directly written glass photonics, IEEE J. Sel. Top. Quant. Electron. 14 (2008) 1370–1381, https://doi.org/10.1109/JSTQE.2008.925809.
[67] B. Gao, T. Chen, W. Cui, C. Li, J. Si, X. Hou, Processing grating structures on surfaces of wide-bandgap semiconductors using femtosecond laser and phase mask, Opt. Eng. 54 (2015) 126106, https://doi.org/10.1117/1.OE.54.12.126106.
[68] Fang Wang, Wu An, Cai Qi, Guo, Laser machining fundamentals: micro, nano, atomic and close-to-atomic scales, IJEM 5 (2023) 012005, https://doi.org/10.1088/2631-7990/acb134.
[69] S. Song, Q. Lu, P. Zhang, H. Yan, H. Shi, Z. Yu, T. Sun, Z. Luo, Y. Tian, A critical review on the simulation of ultra-short pulse laser-metal interactions based on a two-temperature model (TTM), Opt Laser. Technol. 159 (2023) 109001, https://doi.org/10.1016/j.optlastec.2022.109001.
[70] M. DiDomenico Jr., Small-signal analysis of internal (Coupling-Type) modulation of lasers, J. Appl. Phys. 35 (2004) 2870–2876, https://doi.org/10.1063/1.1713121.
[71] W. Li, R. Zhang, Y. Liu, C. Wang, J. Wang, X. Yang, L. Cheng, Effect of different parameters on machining of SiC/SiC composites via pico-second laser, Appl. Surf. Sci. 364 (2016) 378–387, https://doi.org/10.1016/j.apsusc.2015.12.089.
[72] S.C. Feng, C.Z. Huang, J. Wang, H.T. Zhu, P. Yao, L. Wang, A comparison among dry laser ablation and some different water-laser Co-machining processes of single crystal silicon carbide, MSF 861 (2016) 3–8. https://doi.org/10.4028/www.scientific.net/MSF.861.3.
[73] C. Kunka, A. Trachet, G. Subhash, Interaction of indentation-induced cracks on single-crystal silicon carbide, J. Am. Ceram. Soc. 98 (2015) 1891–1897, https://doi.org/10.1111/jace.13525.
[74] T. Fujita, Y. Izumi, J. Watanabe, Ultrafine ductile-mode dicing technology for SiC substrate with metal film using PCD blade, Journal of Advanced Mechanical Design, Systems, and Manufacturing 13 (2019), https://doi.org/10.1299/jamdsm.2019jamdsm0073. JAMDSM0073–JAMDSM0073.
[75] S. Han, H. Yu, C. He, S. Zhao, C. Ning, L. Jiang, X. Lin, Laser slicing of 4H-SiC wafers based on picosecond laser-induced micro-explosion via multiphoton processes, Opt Laser. Technol. 154 (2022) 108323, https://doi.org/10.1016/j.optlastec.2022.108323.
[76] A. Nakajima, Y. Tateishi, H. Murakami, H. Takahashi, M. Ota, R. Kosugi, T. Mitani, S. Nishizawa, H. Ohashi, High-speed dicing of SiC wafers by femtosecond pulsed laser, Mater. Sci. Forum 821–823 (2015) 524–527. https://doi.org/10.4028/www.scientific.net/MSF.821-823.524.
[77] B. Pecholt, S. Gupta, Picosecond pulsed laser ablation and micromachining of 4H–SiC wafers, Appl. Surf. Sci. 255 (2009) 4515–4520, https://doi.org/10.1016/j.apsusc.2008.11.071.
[78] Y. Guo, Y. Zhang, J. Yan, X. Chen, S. Zhang, H. Xie, P. Liu, H. Zhu, J. Wang, J. Li, Sapphire substrate sidewall shaping of deep ultraviolet light-emitting diodes by picosecond laser multiple scribing, Appl. Phys. Express 10 (2017) 062101, https://doi.org/10.7567/APEX.10.062101.
[79] D.O. Bracher, E.L. Hu, Fabrication of high-Q nanobeam photonic crystals in epitaxially grown 4H-SiC, Nano Lett. 15 (2015) 6202–6207, https://doi.org/10.1021/acs.nanolett.5b02542.
[80] E. Ohmura, F. F, K. Fukumitsu, H. Morita, Internal modified-layer formation mechanism into silicon with nanosecond laser, Journal of Achievements in Materials and Manufacturing Engineering 17 (2006), https://doi.org/10.1299/kikaic.74.446.
[81] M. Kumagai, N. Uchiyama, E. Ohmura, R. Sugiura, K. Atsumi, K. Fukumitsu, Advanced dicing technology for semiconductor wafer—stealth dicing, IEEE Trans. Semicond. Manuf. 20 (2007) 259–265, https://doi.org/10.1109/TSM.2007.901849.
[82] E. Kim, Y. Shimotsuma, M. Sakakura, K. Miura, 4H-SiC wafer slicing by using femtosecond laser double-pulses, Opt. Mater. Express 7 (2017) 2450, https://doi.org/10.1364/OME.7.002450.
[83] K.O. Dohnke, K. Kaspar, D. Lewke, Comparison of different novel chip separation methods for 4H-SiC, MSF 821–823 (2015) 520–523. https://doi.org/10.4028/www.scientific.net/MSF.821-823.520.
[84] Z. Zhang, Z. Wen, H. Shi, Q. Song, Z. Xu, M. Li, Y. Hou, Z. Zhang, Dual laser beam asynchronous dicing of 4H-SiC wafer, Micromachines 12 (2021) 1331. https://doi.org/10.3390/mi12111331.
[85] L. Wang, C. Zhang, F. Liu, H. Zheng, G.J. Cheng, Ultrafast pulsed laser stealth dicing of 4H-SiC wafer: structure evolution and defect generation, J. Manuf. Process. 81 (2022) 562–570, https://doi.org/10.1016/j.jmapro.2022.06.064.
[86] B. Yang, H. Wang, S. Peng, Q. Cao, Precision layered stealth dicing of SiC wafers by ultrafast lasers, Micromachines 13 (2022) 1011, https://doi.org/10.3390/mi13071011.
[87] Q. Wen, Y. Yang, J. Lu, H. Huang, C. Cui, Study on picosecond laser stealth dicing of 4H-SiC along [112¯0] and [11¯00] crystal orientations on Si-face and C-face, Opt Laser. Technol. 162 (2023) 109300, https://doi.org/10.1016/j.optlastec.2023.109300.
[88] J. Hattori, Y. Ito, H. Jo, N. Sugita, High-speed observation of damage generation during ultrashort pulse laser drilling of wide-bandgap materials, Laser Applications in Microelectronic and Optoelectronic Manufacturing (LAMOM) XXVI (2021) 137–141, https://doi.org/10.1117/12.2577033. SPIE.
[89] J. Hattori, Y. Ito, H. Jo, K. Nagato, N. Sugita, High-speed observation of pulse energy and pulse width dependences of damage generation in SiC during ultrashort pulse laser drilling, Appl. Phys. A 126 (2020) 861, https://doi.org/10.1007/s00339-020-04018-y.
[90] J. Hattori, Y. Ito, K. Nagato, N. Sugita, Investigation of damage generation process by stress waves during femtosecond laser drilling of SiC, Precis. Eng. 72 (2021) 789–797, https://doi.org/10.1016/j.precisioneng.2021.08.006.
[91] H. Xu, W. Qian, Y. Hua, Y. Ye, F. Dai, J. Cai, Effects of micro texture processed by picosecond laser on hydrophobicity of silicon carbide, J. Inorg. Mater. 38 (2023) 923, https://doi.org/10.15541/jim20230073.
[92] R.L. Fork, B.I. Greene, C.V. Shank, Generation of optical pulses shorter than 0.1 psec by colliding pulse mode locking, Appl. Phys. Lett. 38 (1981) 671–672, https://doi.org/10.1063/1.92500.
[93] R. Miyagawa, O. Eryu, Surface characterization of 6H-SiC substrate irradiated by femtosecond laser, Jpn. J. Appl. Phys. 54 (2015) 071302, https://doi.org/10.7567/JJAP.54.071302.
[94] G.L. DesAutels, C. Brewer, M. Walker, S. Juhl, M. Finet, S. Ristich, M. Whitaker, P. Powers, Femtosecond laser damage threshold and nonlinear characterization in bulk transparent SiC materials, J. Opt. Soc. Am. B, JOSAB 25 (2008) 60–66, https://doi.org/10.1364/JOSAB.25.000060.
[95] V. Khuat, Y. Ma, J. Si, T. Chen, F. Chen, X. Hou, Fabrication of through holes in silicon carbide using femtosecond laser irradiation and acid etching, Appl. Surf. Sci. 289 (2014) 529–532, https://doi.org/10.1016/j.apsusc.2013.11.030.
[96] B. Gao, T. Chen, V. Khuat, J. Si, Hou, Fabrication of grating structures on silicon carbide by femtosecond laser irradiation and wet etching, Chin. Opt Lett. 14 (2016) 21407–21410, https://doi.org/10.3788/COL201614.021407.
[97] B. Meng, J. Zheng, D. Yuan, S. Xu, Machinability improvement of silicon carbide via femtosecond laser surface modification method, Appl. Phys. A 125 (2019), https://doi.org/10.1007/s00339-018-2377-8.
[98] P. Godignon, SiC materials and technologies for sensors development, MSF 483–485 (2005) 1009–1014. https://doi.org/10.4028/www.scientific.net/MSF.483-485.1009.
[99] Y. Chen, Z. Li, D. Shi, S. Dong, X. Chen, J. Gao, Silicon carbide nano-via arrays fabricated by double-sided metal-assisted photochemical etching, Mater. Today Commun. 35 (2023) 105519. https://doi.org/10.1016/j.mtcomm.2023.105519.
[100] Y. Chen, P. Yu, Y. Zhong, D. Shankun, M. Hou, H. Liu, X. Chen, J. Gao, C.-P. Wong, Review—progress in electrochemical etching of third-generation

semiconductors, ECS Journal of Solid State Science and Technology 12 (2023), https://doi.org/10.1149/2162-8777/acce03.
[101] J. Lu, S. Zhan, B. Liu, Y. Zhao, Plasma-enabled electrochemical jet micromachining of chemically inert and passivating material, Int. J. Extrem. Manuf. 4 (2022) 045101, https://doi.org/10.1088/2631-7990/ac84b3.
[102] Y. Huang, F. Tang, Z. Guo, X. Wang, Accelerated ICP etching of 6H-SiC by femtosecond laser modification, Appl. Surf. Sci. 488 (2019) 853–864, https://doi.org/10.1016/j.apsusc.2019.05.262.
[103] X. Xie, Q. Peng, G. Chen, J. Li, J. Long, G. Pan, Femtosecond laser modification of silicon carbide substrates and its influence on CMP process, Ceram. Int. 47 (2021) 13322–13330, https://doi.org/10.1016/j.ceramint.2021.01.188.
[104] K. Sugioka, Femtosecond laser three-dimensional micro- and nanofabrication, J. Appl. Phys. 1 (2014) 041303, https://doi.org/10.1063/1.4904320.
[105] M. Farsari, G. Filippidis, S. Zoppel, G.A. Reider, C. Fotakis, Efficient femtosecond laser micromachining of bulk 3C-SiC, J. Micromech. Microeng. 15 (2005) 1786–1789, https://doi.org/10.1088/0960-1317/15/9/022.
[106] C. Li, X. Shi, J. Si, T. Chen, F. Chen, S. Liang, Z. Wu, X. Hou, Alcohol-assisted photoetching of silicon carbide with a femtosecond laser, Opt Commun. 282 (2009) 78–80, https://doi.org/10.1016/j.optcom.2008.09.072.
[107] W. Wang, H. Song, K. Liao, X. Mei, Water-assisted femtosecond laser drilling of 4H-SiC to eliminate cracks and surface material shedding, Int. J. Adv. Manuf. Technol. 112 (2021) 553–562, https://doi.org/10.1007/s00170-020-06262-1.
[108] B. Liu, P. Fan, H. Song, K. Liao, W. Wang, Fabrication of 4H–SiC microvias using a femtosecond laser assisted by a protective layer, Opt. Mater. 123 (2022) 111695, https://doi.org/10.1016/j.optmat.2021.111695.
[109] H. Song, L. Kai, X. Mei, Water-assisted femtosecond laser drilling of 4H-SiC to eliminate cracks and surface material shedding, Int. J. Adv. Des. Manuf. Technol. 112 (2021) 1–10, https://doi.org/10.1007/s00170-020-06262-1.
[110] Y. Dong, R. Nair, R. Molian, P. Molian, Femtosecond-pulsed laser micromachining of a 4H–SiC wafer for MEMS pressure sensor diaphragms and via holes, J. Micromech. Microeng. 18 (2008) 035022, https://doi.org/10.1088/0960-1317/18/3/035022.
[111] J. Zehetner, G. Vanko, J. Dzuba, I. Ryger, T. Lalinsky, M. Benkler, M. Lucki, Laser ablation for membrane processing of AlGaN/GaN- and micro structured ferroelectric thin film MEMS and SiC pressure sensors for extreme conditions. https://doi.org/10.1117/12.2179041, 2015.
[112] J. Zehetner, S. Kraus, M. Lucki, G. Vanko, J. Dzuba, T. Lalinsky, Manufacturing of membranes by laser ablation in SiC, sapphire, glass and ceramic for GaN/ferroelectric thin film MEMS and pressure sensors, Microsyst. Technol. 22 (2016), https://doi.org/10.1007/s00542-016-2887-2.
[113] L. Wang, Y. Zhao, Y. Zhao, Y. Yang, T. Gong, L. Hao, W. Ren, Design and fabrication of bulk micromachined 4H-SiC piezoresistive pressure chips based on femtosecond laser technology, Micromachines 12 (2021) 56, https://doi.org/10.3390/mi12010056.
[114] L. Wang, Y. Zhao, Y. Yang, X. Pang, L. Hao, Y. Zhao, Piezoresistive 4H-SiC pressure sensor with diaphragm realized by femtosecond laser, IEEE Sensors J 22 (2022) 11535–11542, https://doi.org/10.1109/JSEN.2022.3174046.
[115] Y. Chen, B. Xie, J. Long, Y. Kuang, X. Chen, M. Hou, J. Gao, S. Zhou, B. Fan, Y. He, Y.-T. Zhang, C.-P. Wong, Z. Wang, N. Zhao, Interfacial laser-induced graphene enabling high-performance Liquid–Solid triboelectric nanogenerator, Adv. Mater. 33 (2021) 2104290, https://doi.org/10.1002/adma.202104290.
[116] W. He, J. Yang, C. Guo, Controlling periodic ripple microstructure formation on 4H-SiC crystal with three time-delayed femtosecond laser beams of different linear polarizations, Opt Express 25 (2017) 5156, https://doi.org/10.1364/OE.25.005156.
[117] R. Zhang, C. Huang, J. Wang, S. Feng, H. Zhu, Evolution of micro/nano-structural arrays on crystalline silicon carbide by femtosecond laser ablation, Mater. Sci. Semicond. Process. 121 (2021) 105299, https://doi.org/10.1016/j.mssp.2020.105299.
[118] J. Chen, X. Xie, Q. Peng, Z. He, W. Hu, Q. Ren, J. Long, Effect of surface roughness on femtosecond laser ablation of 4H-SiC substrates, J. Cent. South Univ. 29 (2022) 3294–3303, https://doi.org/10.1007/s11771-022-5136-0.
[119] Z.U. Rehman, K.A. Janulewicz, Structural transformations in femtosecond laser-processed n-type 4H-SiC, Appl. Surf. Sci. 385 (2016) 1–8, https://doi.org/10.1016/j.apsusc.2016.05.041.
[120] J. Long, Q. Peng, G. Chen, Y. Zhang, X. Xie, G. Pan, X. Wang, Centimeter-scale low-damage micromachining on single-crystal 4H–SiC substrates using a femtosecond laser with square-shaped Flat-Top focus spots, Ceram. Int. 47 (2021) 23134–23143, https://doi.org/10.1016/j.ceramint.2021.05.027.
[121] J. Long, Z. He, D. Ou, Y. Huang, P. Wang, Q. Ren, X. Xie, Formation of dense nanostructures on femtosecond laser-processed silicon carbide surfaces, Surface. Interfac. 28 (2022) 101624, https://doi.org/10.1016/j.surfin.2021.101624.
[122] H. Shi, Q. Song, Y. Hou, S. Yue, Y. Li, Z. Zhang, M. Li, K. Zhang, Z. Zhang, Investigation of structural transformation and residual stress under single femtosecond laser pulse irradiation of 4H–SiC, Ceram. Int. 48 (2022) 24276–24282, https://doi.org/10.1016/j.ceramint.2022.03.063.
[123] K. Hirata, New laser slicing technology named KABRA process enables high speed and high efficiency SiC slicing, in: U. Klotzbach, K. Washio, R. Kling (Eds.), Laser-Based Micro- and Nanoprocessing XII, SPIE, San Francisco, United States, 2018, p. 2, https://doi.org/10.1117/12.2291458.
[124] M. Swoboda, R. Rieske, C. Beyer, A. Ullrich, G. Gesell, J. Richter, Cold split kerf-free wafering results for doped 4H-SiC boules, Mater. Sci. Forum 963 (2019) 10–13. https://doi.org/10.4028/www.scientific.net/MSF.963.10.
[125] H. Wang, Q. Chen, Y. Yao, L. Che, B. Zhang, H. Nie, R. Wang, Influence of surface preprocessing on 4H-SiC wafer slicing by using ultrafast laser, Crystals 13 (2022) 15. https://doi.org/10.3390/cryst13010015.
[126] B. Xu, M. Zou, H. Men, F. Dou, X. Ji, JiaxingTang, research on the invisible cutting method of silicon carbide using femtosecond laser, in: 2023 7th International Conference on Measurement Instrumentation and Electronics (ICMIE), IEEE, Hangzhou, China, 2023, pp. 20–24, https://doi.org/10.1109/ICMIE58417.2023.10295406.
[127] T. Okada, T. Tomita, S. Matsuo, S. Hashimoto, Y. Ishida, S. Kiyama, T. Takahashi, Formation of periodic strained layers associated with nanovoids inside a silicon carbide single crystal induced by femtosecond laser irradiation, J. Appl. Phys. 106 (2009) 054307, https://doi.org/10.1063/1.3211311.
[128] E. Kim, Y. Shimotsuma, M. Sakakura, K. Miura, in: T. Jitsuno, J. Shao, W. Rudolph (Eds.), Ultrashort Pulse Laser Slicing of Semiconductor Crystal, 2016, p. 99831B, https://doi.org/10.1117/12.2235146. Yokohama, Japan.
[129] L. Wang, C. Zhang, F. Liu, H. Zheng, G.J. Cheng, Process mechanism of ultrafast laser multi-focal-scribing for ultrafine and efficient stealth dicing of SiC wafers, Appl. Phys. A 128 (2022) 872, https://doi.org/10.1007/s00339-022-06012-y.
[130] Y. Zhang, X. Xie, Y. Huang, W. Hu, J. Long, Internal modified structure of silicon carbide prepared by ultrafast laser for wafer slicing, Ceram. Int. 49 (2023) 5249–5260, https://doi.org/10.1016/j.ceramint.2022.10.043.
[131] L. DesAutels, P. Powers, C. Brewer, M. Walker, M. Burky, G. Anderson, Optical temperature sensor and thermal expansion measurement using a femtosecond micromachined grating in 6H-SiC, Appl. Opt. 47 (2008) 3773–3777, https://doi.org/10.1364/AO.47.003773.
[132] S.H. Kim, I.-B. Sohn, S. Jeong, Fabrication of uniform nanogrooves on 6H-SiC by femtosecond laser ablation, Appl. Phys. A 102 (2011) 55–59, https://doi.org/10.1007/s00339-010-6077-2.
[133] Y. Guo, P. Qiu, S. Xu, G.J. Cheng, Laser-induced microjet-assisted ablation for high-quality microfabrication, Int. J. Extrem. Manuf. 4 (2022) 035101, https://doi.org/10.1088/2631-7990/ac6632.
[134] L. Wang, Y. Zhao, Y. Yang, M. Zhang, Y. Zhao, Experimental investigation on ablation of 4H-SiC by infrared femtosecond laser, Micromachines 13 (2022) 1291, https://doi.org/10.3390/mi13081291.
[135] R. Zhang, C. Huang, J. Wang, D. Chu, D. Liu, S. Feng, Experimental investigation and optimization of femtosecond laser processing parameters of silicon carbide–based on response surface methodology, Ceram. Int. 48 (2022) 14507–14517, https://doi.org/10.1016/j.ceramint.2022.01.344.
[136] T. Yang, C. Liu, T. Chen, M. Shao, C. Jiang, C. Lu, S. Song, Parameter optimization of RB-SiC polishing by femtosecond laser, Materials 16 (2023) 1582, https://doi.org/10.3390/ma16041582.
[137] Y. Aono, K. Ogawa, A. Hirata, Surface modification of single-crystalline silicon carbide by laser irradiation for microtribological applications, Precis. Eng. 54 (2018) 198–205, https://doi.org/10.1016/j.precisioneng.2018.04.019.
[138] G. li, W. Wang, W. Yang, Y. Lin, H. Wang, Z. Lin, S. Zhou, GaN-based light-emitting diodes on various substrates: a critical review, Reports on Progress in Physics. Physical Society (Great Britain) 79 (2016) 056501, https://doi.org/10.1088/0034-4885/79/5/056501.
[139] S. Weigao, L. Ji, Z. Lin, J. Zheng, Z. Wang, L. Zhang, T. Yan, Low-energy UV ultrafast laser controlled lift-off for high-quality flexible GaN-based device, Adv. Funct. Mater. 32 (2022) 2111920, https://doi.org/10.1002/adfm.202111920.
[140] R. Moser, M. Kunzer, C. Goßler, K. Köhler, W. Pletschen, U. Schwarz, J. Wagner, Laser processing of gallium nitride-based light-emitting diodes with ultraviolet picosecond laser pulses, Opt. Eng. 51 (2012) 4301, https://doi.org/10.1117/1.OE.51.11.114301.
[141] S.-J.C. Chang, L.M. Chang, J.Y. Chen, C.S. Hsu, D.S. Kuo, C.F. Shen, W.-S. Chen, T. K. Ko, GaN-based light-emitting diodes prepared with shifted laser stealth dicing, J. Disp. Technol. 12 (2016) 195–199, https://doi.org/10.1109/JDT.2015.2478598.
[142] T. Passow, M. Kunzer, A. Pfeuffer, M. Binder, J. Wagner, Ultraviolet laser ablation as technique for defect repair of GaN-based light-emitting diodes, Appl. Phys. A 124 (2018) 257, https://doi.org/10.1007/s00339-018-1681-7.
[143] S. Nakashima, K. Sugioka, K. Midorikawa, Fabrication of microchannels in single-crystal GaN by wet-chemical-assisted femtosecond-laser ablation, Appl. Surf. Sci. 255 (2009) 9770–9774, https://doi.org/10.1016/j.apsusc.2009.04.159.
[144] S. Nakashima, Fabrication of high-aspect-ratio nanohole arrays on GaN surface by using wet-chemical-assisted femtosecond laser ablation, Journal of Laser Micro/Nanoengineering 6 (2011) 15–19, https://doi.org/10.2961/jlmn.2011.01.0004.
[145] X.C. Wang, G.C. Lim, F.L. Ng, W. Liu, S.J. Chua, Femtosecond pulsed laser-induced periodic surface structures on GaN/sapphire, Appl. Surf. Sci. 252 (2005) 1492–1497, https://doi.org/10.1016/j.apsusc.2005.02.142.
[146] G. Miyaji, K. Miyazaki, Fabrication of 50-nm period gratings on GaN in air through plasmonic near-field ablation induced by ultraviolet femtosecond laser pulses, Opt Express 24 (2016) 4648, https://doi.org/10.1364/OE.24.004648.
[147] N. Yulianto, S. Bornemann, L. Daul, C. Margenfeld, I.M. Clavero, N. Majid, L. Koenders, W. Daum, A. Waag, H.S. Wasisto, Transferable substrateless GaN LED chips produced by femtosecond laser lift-off for flexible sensor applications, in: EUROSENSORS 2018, MDPI, 2018, p. 891, https://doi.org/10.3390/proceedings2130891.
[148] N. Bochkareva Vladislav, R. Gorbunov, A. Zubrilov, V. Kogotkov, P. Latyshev, Y. Lelikov, A. Leonidov, Y. Shreter, Laser slicing: a thin film lift-off method for

GaN-on-GaN technology, Results Phys. 13 (2019) 102233, https://doi.org/10.1016/j.rinp.2019.102233.
[149] L.K. Nolasco, G.F.B. Almeida, T. Voss, C.R. Mendonça, Femtosecond laser micromachining of GaN using different wavelengths from near-infrared to ultraviolet, J. Alloys Compd. 877 (2021) 160259, https://doi.org/10.1016/j.jallcom.2021.160259.
[150] B. Rethfeld, D. Ivanov, M. Garcia, S. Anisimov, Modelling ultrafast laser ablation, J. Phys. Appl. Phys. 50 (2017) 193001, https://doi.org/10.1088/1361-6463/50/19/193001.